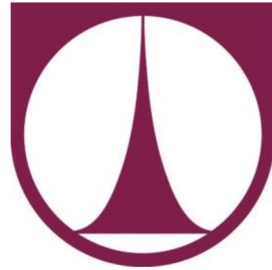


TECHNICAL UNIVERSITY OF LIBEREC

Faculty of Textile Engineering



MASTER THESIS

Liberec 2023

Thi Diem Trang Nguyen



Master Thesis

Preparation and Characterization of Membranes Formed by Non-Solvent Induced Phase Separation Technique.

Study programme: N0723A270002 Textile Engineering

Author: **Thi Diem Trang Nguyen, B.A.**

Thesis Supervisors: doc. Fatma Yalcinkaya, MSc. Ph.D.
Institute of Mechatronics and Computer Engineering

Liberec 2023



Master Thesis Assignment Form

Preparation and Characterization of Membranes Formed by Non-Solvent Induced Phase Separation Technique.

Name and surname: **Thi Diem Trang Nguyen, B.A.**
Identification number: T20000310
Study programme: N0723A270002 Textile Engineering
Assigning department: Department of Nonwovens and Nanofibrous materials
Academic year: 2021/2022

Rules for Elaboration:

Non-solvent induced phase separation (NIPS) is a typical way to prepare asymmetric microstructure membranes. In this process, a polymer solution is laid on a support material and immersed in a non-solvent bath (coagulation bath) where the solvent and non-solvent exchange occurs. Generally, water is used as a non-solvent. The solvent migrates from the polymer solution to the coagulation bath, while the non-solvent follows the reverse path, leading to porous membranes. It is possible to use various polymeric membranes.

In this thesis, microporous polyvinylidene fluoride (PVDF) membranes will be prepared using non-solvent induced phase separation (NIPS) technique. First, the solution concentration will be optimized. Then, using hydrophilic additives such as polyvinylpyrrolidone (PVP) and polyethylene glycol (PEG) polymers at various concentrations will be added into the polymeric solution to improve membrane flux.

The aim is to have an optimal membrane that achieves high membrane flux and permeability.

The characterization will include:

- SEM
- FT-IR (Fourier-transform infrared spectroscopy)
- Filtration device for permeability and flux measurement
- Thickness measurement
- Porosity
- Water contact angle

Expected result:

- Optimized PVDF microporous membrane prepared by NIPS technique
- Understanding the concentration effect on polymeric membrane structure and water permeability
- High membrane flux and permeability

Scope of Graphic Work:

Scope of Report:

Thesis Form: printed/electronic

Thesis Language: English

List of Specialised Literature:

Kahrs C, Schwellenbach J. Membrane formation via non-solvent induced phase separation using sustainable solvents: A comparative study. *Polymer*. 2020 Jan 9;186:122071.

Garcia JU. Understanding Membrane Formation in Nonsolvent-Induced Phase Separation. University of California, Santa Barbara; 2020.

Cao XH, Qiu M, Qin AW, He CJ, Wang HF. Effect of additive on the performance of PVDF membrane via non-solvent induced phase separation. In *Materials Science Forum 2014* (Vol. 789, pp. 240-248). Trans Tech Publications Ltd.

Coveney S. *Fundamentals of Phase Separation in Polymer Blend Thin Films*. Springer; 2015 Jun 18.

Thesis Supervisors: doc. Fatma Yalcinkaya, MSc. Ph.D.
Institute of Mechatronics and Computer Engineering

Date of Thesis Assignment: November 1, 2021

Date of Thesis Submission: May 16, 2022

L.S.

doc. Ing. Vladimír Bajzík, Ph.D.
Dean

doc. Ing. Jiří Chvojka, Ph.D.
Head of Department

Liberec November 1, 2021

Declaration

I hereby certify, I, myself, have written my master thesis as an original and primary work using the literature listed below and consulting it with my thesis supervisor and my thesis counsellor.

I acknowledge that my master thesis is fully governed by Act No. 121/2000 Coll., the Copyright Act, in particular Article 60 – School Work.

I acknowledge that the Technical University of Liberec does not infringe my copyrights by using my master thesis for internal purposes of the Technical University of Liberec.

I am aware of my obligation to inform the Technical University of Liberec on having used or granted license to use the results of my master thesis; in such a case the Technical University of Liberec may require reimbursement of the costs incurred for creating the result up to their actual amount.

At the same time, I honestly declare that the text of the printed version of my master thesis is identical with the text of the electronic version uploaded into the IS/STAG.

I acknowledge that the Technical University of Liberec will make my master thesis public in accordance with paragraph 47b of Act No. 111/1998 Coll., on Higher Education Institutions and on Amendment to Other Acts (the Higher Education Act), as amended.

I am aware of the consequences which may under the Higher Education Act result from a breach of this declaration.

January 3, 2023

Thi Diem Trang Nguyen, B.A.

- Abstrakt

Na základě vynikajících výhod polymerní membrány jsou v této práci připraveny porézní membrány metodou NIPS (separace fází indukované rozpouštědlem), které mají obecně asymetrickou strukturu. Membrány měly póry o velikosti mikronů, které se nazývají mikrofiltry, a byly použity pro separaci mikroplastů.

Bylo připraveno 21 různých membrán s různou koncentrací PVDF nebo PVP nebo PEG. Homopolymer PVDF byl smíchán s příměsí PVP a PEG a zkoumán z hlediska morfologie a velikosti pórů pomocí SEM obrazu, chemických vlastností pomocí FTIR, jejich hydrofilnosti a filtračních vlastností pomocí kontaktního úhlu, transportního toku, propustnosti, absorpce vody a míry rejekce, jakož i jejich stability pomocí poměru bobtnání.

V této studii by metoda NIPS mohla podpořit tvorbu asymetrické membrány, zlepšit její transportní médium. Byla zkoumána korelace mezi polymerem a jeho obsahem v dopingovém roztoku a filtračním výkonem. Celkově lze říci, že vlastnosti membrán byly silně závislé na obsahu PVDF i na koncentraci přísad, neboť výsledky jednotlivých charakteristik membrán se lišily.

Přísada PEG měla obecně na konečné vlastnosti směsné membrány PVDF/PEG jen malý vliv, protože se PEG během tvorby membrány vylučoval. Přídavek PVP do směsného systému PVDF/PVP vedl k slibnějším výsledkům, jako je vysoká propustnost vody, a skupina membrán PVDF10/PVP vykazovala nejlepší výsledky mezi vyrobenými membránami. Naopak míra rejekce membrány při filtraci nebyla dostatečně dobrá, což mohlo být způsobeno velkým rozložením pórů nebo praskáním povrchu membrány.

Závěrem lze říci, že tato studie prokázala potenciální výhodu porézní tenké vrstvy vytvořené metodou NIPS a také slibný výsledek přimícháním přísady PVP do systému PVDF při tvorbě membrán.

Klíčová slova: NIPS, porézní membrána, PVDF membrána, PVP přísada, PEG přísada, filtrace.

- Abstracts

Based on the superior advantages of the polymeric membrane, this thesis is prepared porous membranes with the Non-solvent induced phase separation (NIPS) method which generally has an asymmetric structure. The membranes had micron size pores which are called microfilters and were used for the separation of microplastics.

Twenty-one different membranes by varying concentration of PVDF or PVP or PEG were prepared. PVDF homopolymer was blended with PVP and PEG additive and investigated in terms of morphology and pore size by SEM image, chemical property by FTIR, their hydrophilicity and filtration performance by contact angle, transport flux, permeability, water uptake and rejection rate, as well as their stability by swelling ratio.

In this study, NIPS method could support to form the asymmetric membrane, enhance its transport media. The correlation between polymer and its content in dope solution and filtration performance was investigated. Overall, the membrane properties had strongly dependent on PVDF content as well as additives concentration since each membrane's characterization varied in results.

Generally, PEG additive contributed minor effect to final property of blended PVDF/PEG membrane due to PEG leaching out during membrane formation. Adding PVP to blended PVDF/PVP system resulted in more promising outcome such as high water permeability, and PVDF10/PVP membrane group performed the best among fabricated membranes. On the contrary, the membrane rejection rate was not good enough in filtration, it could be because of large pores distribution or membrane surface cracking.

In conclusion, this study demonstrated the potential advantage of porous thin film created by NIPS method as well as the promising outcome by blending PVP additive in PVDF system during membrane formation.

Keywords: NIPS, porous membrane, PVDF membrane, PVP additive, PEG additive, filtration.

- Table of content

- Abstracts.....	1
- Table of content.....	2
- List of Figures	4
- List of Tables.....	5
- Nomenclature	6
1 Introduction	7
2 Literature Review	9
2.1 Membrane	9
2.1.1 Membrane technology	9
2.1.2 Asymmetric membrane.....	11
2.1.3 Microfiltration membrane.....	12
2.1.4 Microfiltration membrane material.....	13
2.2 Phase inversion techniques	14
2.2.1 Asymmetric membrane preparation.....	14
2.2.2 Phase inversion techniques	15
2.2.2.1 Thermally Induced Phase Separation.....	18
2.2.2.2 Non – solvent Induced Phase Separation.....	18
2.2.2.3 Drying Induced Phase Separation	19
2.2.2.4 Vapour Induced Phase Separation	19
2.3 Polymeric solution.....	19
2.3.1 Characteristic of PVDF as a membrane material.....	19
2.3.1.1 Crystalline property of PVDF.....	19
2.3.1.2 Thermal stability property of PVDF	22
2.3.1.3 Chemical resistance property of PVDF	24
2.3.2 Characteristic of DMAc as polymeric solvent.....	25
2.3.3 Characteristic of polymeric additives.....	26
2.3.3.1 Characteristic of PVP as a polymeric additive.....	27
2.3.3.2 Characteristic of PEG as a polymeric additive	28
2.4 Membranes preparation	29
3 Materials, Apparatus, and Procedures	30
3.1 Characteristics of used chemicals.....	30

3.2	Polymeric solution preparation	30
3.3	Membrane preparation by NIPS technique.....	31
3.4	Membrane characterization	32
3.4.1	Fourier transform infrared spectroscopy	32
3.4.2	Membrane pore diameter and membrane thickness	33
3.4.3	Contact angle.....	33
3.4.4	Water uptake and swelling degree of membrane	35
3.4.5	Filtration test.....	36
3.4.5.1	Preparation of feed solution with microplastics	36
3.4.5.2	Turbidity.....	36
3.4.5.3	Amicon dead-end filtration unit.....	38
3.4.5.4	Calculation of flux, permeability and particle rejection rate.....	39
4	Results and Discussion	41
4.1	Membrane morphology by SEM images.....	41
4.2	FTIR	46
4.3	Membrane pore size and membrane thickness	52
4.4	Contact angle.....	53
4.5	Permeability and rejection rate	56
4.5.1	Water permeability performance for all membranes.....	56
4.5.2	Permeability performance and rejection rate of selected membranes by different pollutant solutions.....	64
4.6	Water uptake and swelling degree	68
5	Conclusion and Recommendations.....	70
-	Bibliography	72
-	Appendixes	79
	Appendix A: Pore dimension measurement of fabricated membranes.	79
	Appendix B: Membrane thickness measurement of fabricated membranes.	79

- List of Figures

Figure 2-1 Membrane separation processes and classifications of sizes of solutes and particles.	11
Figure 2-2 Schematic of a membrane filtration process.	12
Figure 2-3 Schematic of a phase inversion process.	15
Figure 2-4 Schematic of ternary phase diagram in phase inversion	17
Figure 2-5 Schematic of non – solvent induced phase separation process.	18
Figure 2-6 Chemical structure of PVDF	20
Figure 2-7 Structures of α , β , and γ PVDF phase.	21
Figure 2-8 TGA thermograms of halogen-containing polymers in air	23
Figure 2-9 Dehydrofluorodion reaction in PVDF by (a) formation of double bond and (b) cross-linking of polymer.	24
Figure 2-10 Chemical structure of DMAc.	25
Figure 2-11 Non-solvent phase inversion casting process	26
Figure 2-12 Chemical structure of PVP	27
Figure 2-13 Chemical structure of PEG	28
Figure 3-1 Schematic of NIPS process on lab – scale.	32
Figure 3-2 Schematic of a sessile–drop contact angle system.	34
Figure 3-3 The advancing and the receding contact angle	34
Figure 3-4 Surface wetting ability classification by contact angle	35
Figure 3-5 Turbidimeter TB300 IR model.	38
Figure 3-6 (a, b) Amicon Stirred Cell components and (c) dead end filtration cell schematic.	39
Figure 4-1 Surface morphology of pristine PDVF membranes by SEM images: a) PVDF10 b) PVDF15 c) PVDF20.	41
Figure 4-2 Cross-section of pristine PDVF membranes by SEM images: a) PVDF10 b) PVDF15 c) PVDF20.	41
Figure 4-3 Surface morphology of blended PDVF with PVP additive membranes by SEM images: a) PVDF10/PVP2 b) PVDF10/PVP5 c) PVDF10/PVP8 d) PVDF15/PVP2 e) PVDF15/PVP5 f) PVDF15/PVP8 g) PVDF20/PVP2 h) PVDF20/PVP5 i) PVDF20/PVP8.	42
Figure 4-4 Cross-section of blended PDVF with PVP additive membranes by SEM images: a) PVDF10/PVP2 b) PVDF10/PVP5 c) PVDF10/PVP8 d) PVDF15/PVP2 e) PVDF15/PVP5 f) PVDF15/PVP8 g) PVDF20/PVP2 h) PVDF20/PVP5 i) PVDF20/PVP8.	43
Figure 4-5 Surface morphology of blended PDVF with PEG additive membranes by SEM images: a) PVDF10/PEG2 b) PVDF10/PEG5 c) PVDF10/PEG8 d) PVDF15/PEG2 e) PVDF15/PEG5 f) PVDF15/PEG8 g) PVDF20/PEG2 h) PVDF20/PEG5 i) PVDF20/PEG8.	44
Figure 4-6 Cross-section of blended PDVF with PEG additive membranes by SEM images: a) PVDF10/PEG2 b) PVDF10/PEG5 c) PVDF10/PEG8 d) PVDF15/PEG2 e) PVDF15/PEG5 f) PVDF15/PEG8 g) PVDF20/PEG2 h) PVDF20/PEG5 i) PVDF20/PEG8.	45
Figure 4-7 FTIR spectra of pristine PVDF membrane.	47
Figure 4-8 FTIR spectra of PVDF10/PVP membranes.	48
Figure 4-9 FTIR spectra of PVDF15/PVP membranes.	48
Figure 4-10 FTIR spectra of PVDF20/PVP membranes.	49
Figure 4-11 FTIR spectra of PVDF10/PEG membranes.	50

Figure 4-12 FTIR spectra of PVDF15/PEG membranes.....	50
Figure 4-13 FTIR spectra of PVDF20/PEG membranes	51
Figure 4-14 Water permeability of PVDF10 group.	60
Figure 4-15 Water permeability of PVDF15 group.	61
Figure 4-16 Water permeability of PVDF20 group.	62

- List of Tables

Table 2-1 Membrane separation processes in industrial practice	9
Table 2-2 Thermal stability of frequently used polymer in membrane industry	23
Table 3-1 Composition of the polymeric solution.	30
Table 3-2 Components of the feed solution.	36
Table 3-3 Turbidity of DI water and feed solution.	38
Table 4-1 Average pore diameter data.	52
Table 4-2 Contact angle data with images.	54
Table 4-3 Water permeate flux data.	57
Table 4-4 Water permeability performance data.	59
Table 4-5 Permeability performance of selected membranes by water-soluble pollutants with 0.1µm diameter.	65
Table 4-6 Permeability performance of selected membranes by water-soluble pollutants with 0.2µm diameter.	65
Table 4-7 Permeability performance of selected membranes by water-soluble pollutants with 0.5µm diameter.	66
Table 4-8 Permeability performance and rejection rate of selected membranes by water-soluble pollutants solution.	67
Table 4-9 Water uptake data.....	68
Table 4-10 Swelling degree data	68
Table 0-1 Thickness measurement of PVDF10.....	79
Table 0-2 Thickness measurement of PVDF10/PVP2.....	79
Table 0-3 Thickness measurement of PVDF10/PVP5.....	79
Table 0-4 Thickness measurement of PVDF10/PVP8.....	80
Table 0-5 Thickness measurement of PVDF10/PEG2.....	80
Table 0-6 Thickness measurement of PVDF10/PEG5.....	80
Table 0-7 Thickness measurement of PVDF10/PEG8.....	81
Table 0-8 Thickness measurement of PVDF15.....	81
Table 0-9 Thickness measurement of PVDF15/PVP2.....	81
Table 0-10 Thickness measurement of PVDF15/PVP5.....	82
Table 0-11 Thickness measurement of PVDF15/PVP8.....	82
Table 0-12 Thickness measurement of PVDF15/PEG2.....	82
Table 0-13 Thickness measurement of PVDF15/PEG5.....	83
Table 0-14 Thickness measurement of PVDF15/PEG8.....	83
Table 0-15 Thickness measurement of PVDF20.....	83
Table 0-16 Thickness measurement of PVDF20/PVP2.....	84

Table 0-17 Thickness measurement of PVDF20/PVP5.....	84
Table 0-18 Thickness measurement of PVDF20/PVP8.....	84
Table 0-19 Thickness measurement of PVDF20/PEG2.....	85
Table 0-20 Thickness measurement of PVDF20/PEG5.....	85
Table 0-21 Thickness measurement of PVDF20/PEG8.....	85

- Nomenclature

DI	Distilled water	PS	Polysulfone
DIPS	Drying induced phase separation	PSF	Polysulfone
DMAc	N,N-Dimethylacetamide	PTFE	Polytetrafluoroethylene
DMF	Dimethylformamide	PTFE	Polytetrafluoroethylene
DMSO	Dimethyl sulfoxide	PV	Pervaporation
ED	Electrodialysis	PVB	Polyvinyl bromide
FT-IR	Fourier-transform infrared spectroscopy	PVC	Polyvinyl chloride
GS	Gas separation	PVDB	Polyvinylidene bromide
HF	Hydrogen fluoride	PVDC-VC	vinylidene chloride - vinyl chloride copolymer
MBR	Membrane bioreactor	PVDF	Polyvinylidene Fluoride
MF	Microfiltration	PVF	Polyvinyl fluoride
NaCl	Sodium Chloride	PVP	Polyvinylpyrrolidone
NaOH	Sodium hydroxide solution	RO	Reverse osmosis
NF	Nanofiltration	SEM	Scanning electron microscopy
NIPS	Non-solvent induced phase separation	TBA	Torsional Braid Analysis
NMP	N-methyl-2-pyrrolidone	TEP	Tetraethyl phosphate
NTUs	Nephelometric turbidity units	TGA	Thermogravimetric analysis
PA	Polyamide	TIPS	Thermally induced phase separation
PE	Polyethylene	UF	Ultrafiltration
PEG	Polyethylene Glycol	VIPS	Vapour induced phase separation
PES	Polyethersulfone	w/v%	Percent of weight of solution in the total volume of solution
PI	Polyimide	wt%	Weight percentage
PP	Polypropylene	WU	Water uptake value

1 Introduction

The membrane market is recognized to continuously develop from 5.4 billion USD in 2019 to 8.3 billion USD by 2024, at a compounded annual rate of growth of 9.0%. The significant moving for the membrane market is being driven by growing population, increasing mindfulness about wastewater treatment, and fast industrialization. The traditional and costly method for water filtration is building a large treatment plant and chlorinating the contaminated water. To make water treatment more approachable and lower cost, researchers tend to move the chemical mechanism of water purification to physical ones. Due to the superior advantages of the polymer such as cost-effective production and high performance in filtration, polymeric membranes are used in a variety of applications, such as “beverage processing, feed water production, chemical processing, and others”. Based on the MarketsandMarkets™ forecast report in January of 2020, the polymeric membrane is expected to even more dominant position in the membrane market in near future [1].

Polyvinylidene fluoride (PVDF) is well-known for microfiltration and ultrafiltration membranes because of its excellent mechanical strength, superior chemical resistance, and high thermal stability properties [2]. However, its natural hydrophobicity is a drawback for filtration applications. Therefore, modifying the PVDF membrane to enhance its hydrophilicity is one of the issues that need to be tackled and the typical solution is adding a polymeric additive to the PVDF solution. The modified polymeric solution is expected to increase the hydrophilicity in the resulting PVDF membrane.

The flat sheet polymeric membranes are frequently formed via the Non-solvent induced phase separation (NIPS) method. In the process, a polymeric solution is cast on a support screen and immersed in a non-solvent bath, where phase inversion occurs, transforming polymer from liquid to solid phase. During the inversion, the solvent migrates from the polymer solution to the coagulation bath (CB), while the non-solvent follows the reverse path, leading to creating of porous membranes. This exchange induces phase inversion and results in asymmetric microstructure membranes [3,4].

In the range of this thesis, microporous PVDF membranes will be prepared using the NIPS technique on a laboratory – scale. First, the solution concentration will be optimized. Then, hydrophilic additives such as polyvinylpyrrolidone (PVP) and polyethylene glycol (PEG) polymers at various concentrations will be added to the polymeric solution to improve membrane permeability. The aim is to have an optimal membrane that achieves high membrane flux and permeability.

The objective of this study is to evaluate the impact of a blending ratio of PVDF polymer with PVP or PEG additives on filtration performance of resulting membrane during NIPS fabrication. To gain a better understanding of the PVDF membranes and their characteristics, as well as enhance knowledge about the NIPS techniques to create asymmetric membranes, this thesis is

motivated to work on the topic: **Preparation and Characterization of Membranes Formed by Non-Solvent Induced Phase Separation Technique.**

The thesis is separated into 5 chapters, including:

- Chapter 1: Introduction: to introduce the research background as well as the thesis topic.
- Chapter 2: Literature Review: to prepare the theoretical foundation of research and experiment.
- Chapter 3: Materials, Apparatus, and Procedures: to describe membrane-making procedure and methodology for membrane characteristics.
- Chapter 4: Result and Discussion: to present and compare experimental results with theoretical expectations.
- Chapter 5: Conclusion: to summarize the outcomes of research and thesis contribution.

2 Literature Review

2.1 Membrane

2.1.1 Membrane technology

Separation processes have been attributed to the development of the chemical industry, especially in membrane technology. The processes are classified by two techniques, including phase separation and component separation [5].

The phase separation technique occurs when dope solution exchanges at least two different phases. The exchange mechanism is by the physical properties differences, such as solution density, solution viscosity, or average polymeric particles size. The common technologies are sieving, filtration, centrifugation, and flotation [5].

The component separation technique happens when the dope solution is prepared by the difference in vapor pressure, chemical nature, affinity, or freezing point. The common technologies are distillation, drying, extraction, crystallization, and ion exchange [5,6].

It is a long time since the membranes produced by the phase separation technique have been utilized. Membrane for filtration by phase separation technique accomplished an important role in the filtration industry since the first ones were invented in the 1930s, and followed closely manufactured in bulk – scale [5]. While Pfeffer et al. used a membrane produced by component separation technique in an osmotic experiment on sugar solution, the applications of this technique were limited and unnoticed in the early 20th century [7]. Practical performances of component separation technique only took a considerable influence from the 1960s and their applications became widespread lately.

Based on geometric structure, the prepared membranes could be classified by asymmetric membrane and symmetric membrane. Because of the extremely thin surface layer, the filtration performance of the asymmetric membrane is sufficiently high, compared with conventional separation. Its promising benefits also result in less energy required compared with the distillation process or non-solvent required compared with the extraction process. With those improvements, the asymmetric membrane industry saw a significant rise recently [5,8]. The main membrane filtration technology with its characteristics are listed in Table 2-1.

Table 2-1 Membrane separation processes in industrial practice [5,8].

Filtration technology	Membrane type	Driving force	Transport mode	Application
Microfiltration (MF)	Symmetrical or asymmetrical, microporous, thickness: 10 – 150	Pressure difference, $\Delta p = 0.5 - 2$ bar	Sieve effect	The concentration of suspension and emulsion, clarification

	μm , pore diameter: 0.05 – 10 μm			filtration, bacteria removal
Ultrafiltration (UF)	Asymmetric, microporous, thickness: 150 μm , pore diameter: 2 – 100 nm	Pressure difference, Δp = 1 – 10 bar	Sieve effect	Recovery of starch, proteins, and enzymes, whey processing
Nanofiltration (NF)	Asymmetric or composite, the thickness of bottom layer: 150 μm , thickness of top layer: 1 μm , pore diameter < 2 nm	Pressure difference, Δp = 10 – 25 bar (brackish water)	Solution diffusion	Desalination of brackish water, the concentration of whey, recovery of homogeneous catalysts
Reverse osmosis (RO)	Asymmetric or composite, the thickness of bottom layer: 150 μm , top layer thickness: 1 μm , pore diameter < 2 nm	Pressure difference, Δp = 15 – 25 bar (brackish water), 40 – 80 bar (seawater)	Solution diffusion	Desalination of brackish and seawater, production of ultrapure water (semiconductor industry)
Dialysis	Symmetric, dense membranes, thickness: 10 – 100 μm	Concentration difference	Solution diffusion	Alcohol reduction in beer, hemodialysis (artificial kidney)
Electrodialysis (ED)	Symmetric with incorporated ionogenic groups	Electrical potential difference	Electrical potential difference	Desalination of process water
Gas separation (GS)	Composite or asymmetric with dense polymer top layer, thickness of top layer: 0.1 – few μm	Pressure difference, Δp = up to approx. 100 bar, Concentration difference	Solution diffusion	Separation of: hydrogen/nitrogen, Carbon dioxide/methane, Oxygen/nitrogen
Pervaporation (PV)	Composite with the dense separation- active upper layer, Thickness of top layer: 0.1 – few μm	Concentration difference, vapor pressure difference	Solution diffusion	Dehydration of solvents, Concentration of Ethanol

Moreover, based on separation regime, membrane filtration can be divided by various morphological pore structures including microfiltration (MF), ultrafiltration (UF), nanofiltration (NF), reverse osmosis (RO), gas separation (GS), pervaporation (PV), dialysis and electro dialysis (ED) [1]. The phase separation technique commonly produces porous structure material like MF and UF, while the component separation technique deals with denser structure as RO or defect-free structures like GS, PV, and dialysis [6,8].

David et al. introduced the membrane separation processes by the means of particle pore sizes, molecular weight cut-off (MWCO) and examples of sizes of solutes and particles. Moreover, a typical method for using MF and UF membranes for water treatment in different industries is to consolidate them into an imparted sludge process named a membrane bioreactor (MBR) [9].

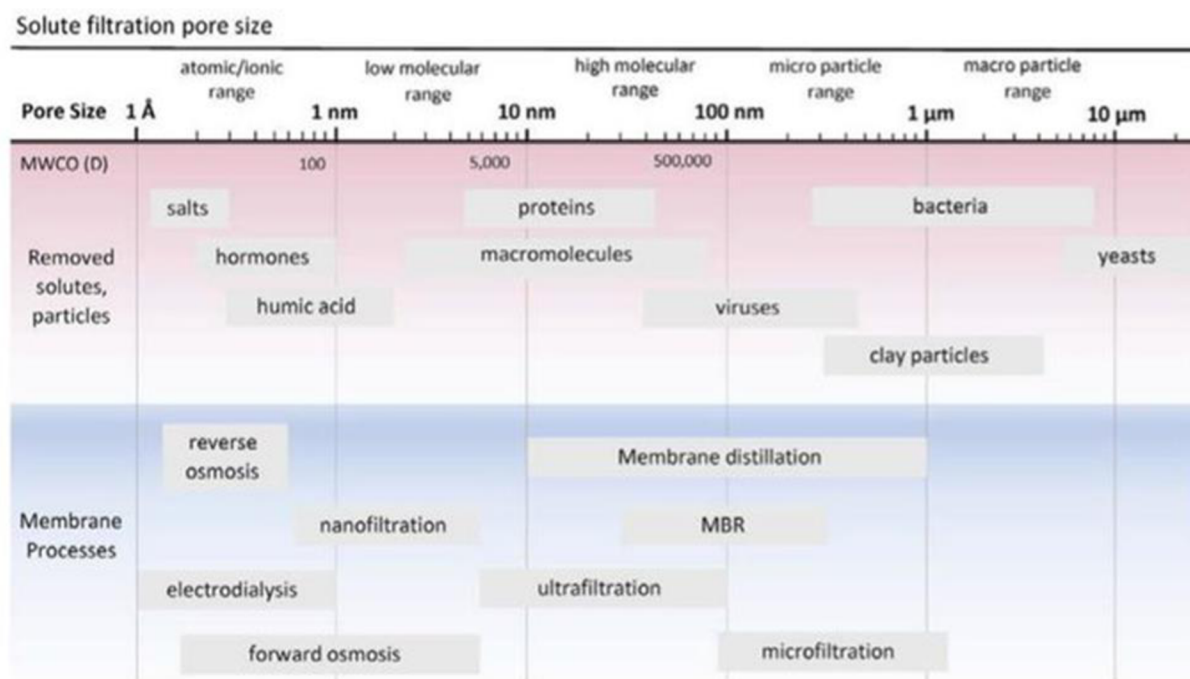


Figure 2-1 Membrane separation processes and classifications of sizes of solutes and particles [9].

This thesis is prepared porous membranes with the NIPs method which generally has an asymmetric structure. The membranes had micron pores size which are called microfilters and were used for the separation of microplastics.

2.1.2 Asymmetric membrane

The thickness of the membrane has a significant impact on its performance and varies inversely with its efficiency: the thinner membrane, the higher its performance. Loeb and Sourirajan introduced a new approach to produce an asymmetric membrane in 1964, which significantly

improved the membrane performance by its morphology. The advantages of their invention were superior to the conventional separation technique, especially in the permeability performance of resulted material. The filter mechanism of a symmetric membrane is using the whole cross-section of the membrane to activate particles separation, while the asymmetric membrane applies a tiny portion of the membrane cross-section (up to $0.5\ \mu\text{m}$) – called a separation – active layer – engages in filtration. The other parts in a cross-section of asymmetric membrane work as a mechanical supporter to the active layer and as a stabilizer of the whole membrane [10]. To conclude, the smaller pore system on the surface of the asymmetric membrane (feed – side) takes account of filtration capabilities while the larger pore system deeper into the membrane is for mechanical support and stability without decreasing the flux speed. Figure 2-2 shows the schematic of a membrane filtration process with three different states, including feeding, permeating, and retentating. The permeating addresses for how much feed solution passing through the membrane, while the retentating addresses for residual particles trapped by the membrane.

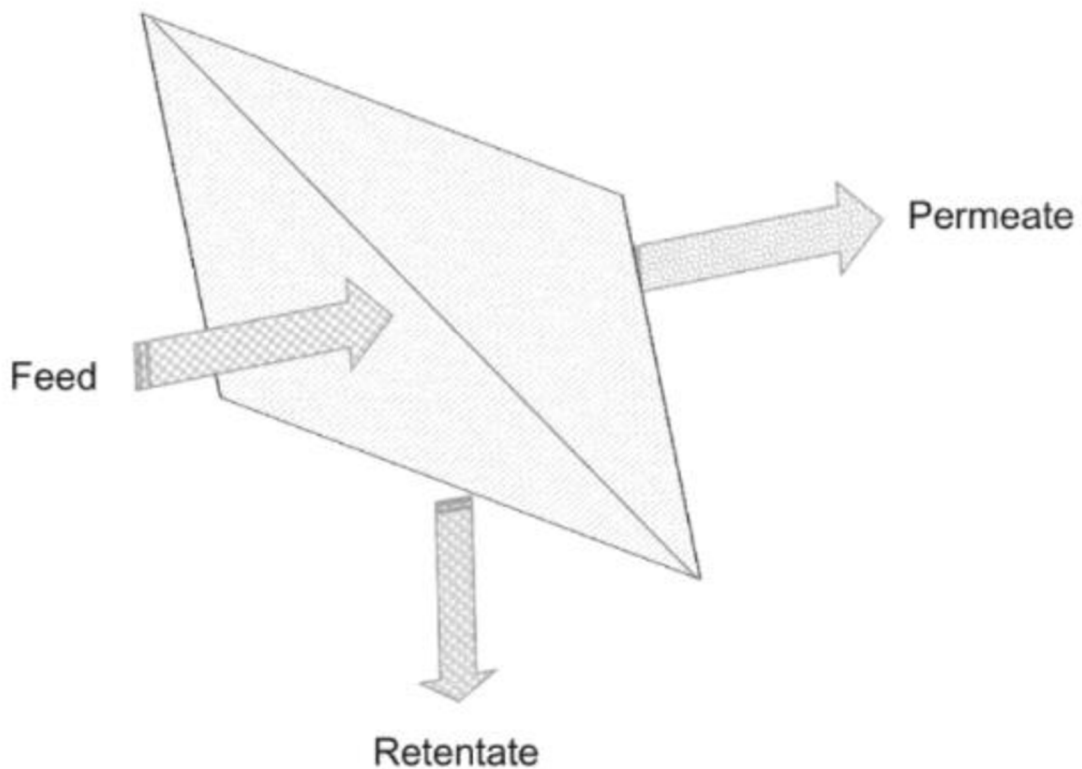


Figure 2-2 Schematic of a membrane filtration process [11].

2.1.3 Microfiltration membrane

According to lacking freshwater, numerous researches have been developed and membrane technology is a typical method to tackle this issue. The advantages of membrane technology are low energy consumption, ease of bulk production, and simple operational parameters [12].

The highlight property of porous membrane is its filter media, relating to selectivity and permeability of the sieving effect. A huge range of membrane applications is developed for water purification, chemical processing, desalination of brackish and seawater, etc. Various types of filtration technology have been used for different purposes and MF is the most commonly used membrane. The external pressure drives the contaminated fluid through the membrane barrier (surface pore system), then particles are retained on one side of the membrane.

Microfiltration is attributed to the development of the membrane industry for effectively filtering contaminated components from a fluid stream by its mechanical mechanism. It is proven that microfiltration can catch up particles with their size are larger than $0.1\ \mu\text{m}$ [5,8], so that can remove colloids and bacteria from the stream. The filtration performance of MF is highly dependent on its microstructure with pore sizes of the surface layer is from 0.05 to $10\ \mu\text{m}$ and thickness of the membrane is from 10 to $150\ \mu\text{m}$.

The remaining large particles on the feed – side of the membrane through the micro-sieving is the most concerned when MF is applied. The membrane surface is overlaid with retaining components which become a gel layer after time, it is the reason for the deceleration of fluid flux and permeability. Surface fouling is also another considerable problem of MF. The filtered particles are deposited or absorbed into the membrane and clog the membrane pores. Surface fouling can cause an intensive decrease in filtered flux and the quality of filtered output. Due to problems occurring in the filtration process, the membrane materials are selected with critical criteria for improving surface hydrophilicity, antifouling performance, and permeability [2].

2.1.4 Microfiltration membrane material

Polymer and inorganic chemicals such as ceramics and metals are frequently used materials to produce MF membranes [13]. The inorganic MF membrane has listed properties:

- Temperature resistance.
- Mechanical stability.
- Chemical resistance.
- Stable pore structure.
- Low flow reduction.
- No aging or long-life service.

Instead of the listed properties above, the production of inorganic MF membrane is interfered with and hard to bring to bulk – scale due to its high-cost manufacturing. In contrast, the polymer-based membrane is easier to commercialize because of its reasonable material cost. When compares with ceramic membrane, polymer MF membrane is lower thermal stability and chemical resistance problems but it also has significant properties listed below [5]:

- Wide chemical variation possibilities of the polymer structure.
- Possibility to realize different shaped bodies.

- High strength-to-weight ratio.
- Easy to customize properties for special applications.
- Flexibility.
- Relatively easy processing.
- Low cost.

Because of the qualities listed above, polymeric membranes are commonly utilized for filtration purposes. Polymeric membranes are frequently made by polysulfone (PSF), polyethersulfone (PES), and PVDF, which have high hydrolytic and thermal stability and good permeability [14].

The main criteria for polymeric membranes are listed below [15] and are strongly dependent on the surface structure and morphology of the membrane.

- Narrow pore size distribution.
- High surface porosity.
- Thin thickness.
- Hydrophilicity or good wettability.
- Chemical resistance to various feed components and cleaning agents.
- High resistance to fouling.
- Thermal stability in the operating temperature range.
- Mechanical stability against applied pressure.
- Low cost.
- Other standards are defined by specific circumstances.

2.2 Phase inversion techniques

2.2.1 Asymmetric membrane preparation

The asymmetric membrane is prepared by two different techniques, including the phase inversion process and composite thin film making [8].

In the phase inversion process, the polymeric solution is prepared by dissolving chosen polymer with an appropriate solvent. Then the solution is cast as a thin film, followed by adding non – solvent for causing precipitating polymer. The liquid thin film transforms into a solid polymer after precipitation and separation solvent, leading to creating a porous membrane. Phase inversion term describes how the polymer exchange from liquid to solid-state and form the membrane matrix [8].

On the other hand, the composite thin film creates an asymmetric membrane by combining two different materials. Composite includes one thin polymer film attached to a porous substructure by solution coating or interfacial polymerization [8].

Asymmetric membrane made by composite thin films method is extremely sensitive with support layer thickness, let it increase the filtration flux. Despite this benefit, composites material cannot

surpass phase inversion membrane in bulk-scale production. Garcia introduced two main reasons for this circumstance [16]:

- Firstly, composite membranes are produced by complicated membrane formation process, therefore it increases the production cost and make it less economic goods.
- Secondly, the membrane performances greatly depend on the porous substructure character and quality, instead of the thin film made by phase inversion.

To conclude, phase inversion techniques are the most common method to fabricate an asymmetric membrane.

2.2.2 Phase inversion techniques

Kesting described phase inversion techniques as exchanging phases of polymer: polymer-rich phase and polymer-poor phase. In polymeric solution, the polymer-rich phase solidifies to form the membrane matrix, and polymer-poor phase simultaneously creates the porous system [17].

A schematic of the phase inversion process was shown in Figure 2-3 [18]:

- a) Polymeric solution is cast over a glass plate (by casting knife) to form a film.
- b) Casted film deposits on a glass plate.
- c) Casted film is partially evaporated or dried from the solvent from the polymeric solution before immersion.
- d) Casted film is immersed in a coagulation bath (CB) and contacted with a non-solvent solution, and the polymer precipitation occurs.
- e) Asymmetric polymeric membrane is created with a top dense skin layer and a porous sublayer.

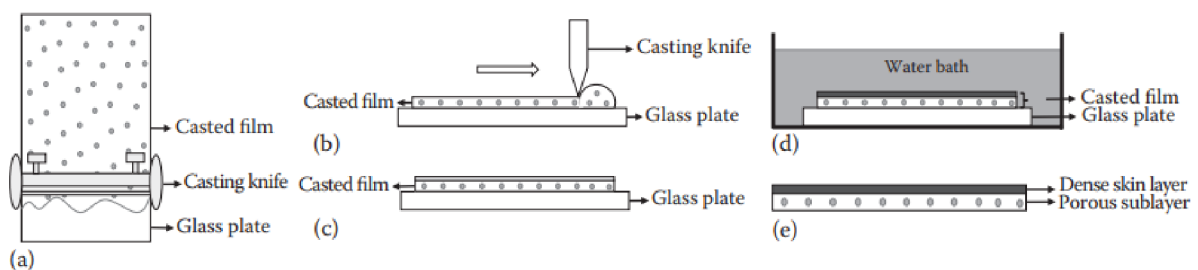


Figure 2-3 Schematic of a phase inversion process [18].

Strathmann and co-workers introduced the triangle to represent the casted solution components, called the ternary phase diagram, including polymer, solvent, and non-solvent factors. The diagram shown the casted film in the homogeneous gel stage, phase separation stage, and solidification stage [8].

“The triangle is divided into two regions:

- The first region represents a one-phase region in which all components present in the system are miscible.
- The second region represents a two-phase region in which the system divides into two phases: (1) a polymer-rich phase (normally solid phase), and (2) a polymer-poor phase (normally liquid phase).

When the quenching of a homogeneous solution of polymer (point A) is done in the precipitant, the composition of polymer or boundary moves along ABC to the two-phase area, one phase is a membrane (a solid porous phase) and another is a liquid phase (pores filling liquid).

At point B, a transition takes place from one phase to the two-phase area in which the mixture breaks into a polymer-rich phase and a polymer-poor phase. The polymer-rich phase becomes solid at point D.

Point C shows the net membrane at which the two-phase region is in equilibrium, where point S is the solid (polymer-rich) phase and point L is the liquid (polymer-poor) phase.

On the line S –L, position C is used to determine the membrane porosity. The solid phase is an asymmetric membrane, which contains a dense surface layer and a porous subsurface layer.” [19]

Figures 2-4 show a ternary phase diagram in phase inversion with water acting like a non-solvent solution.

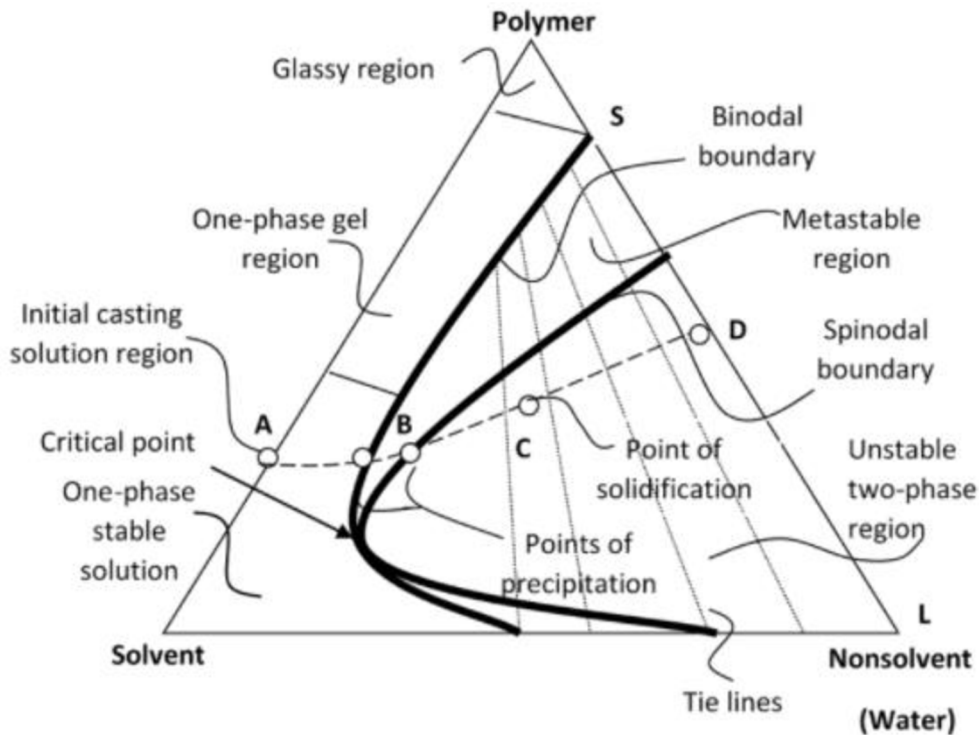


Figure 2-4 Schematic of ternary phase diagram in phase inversion [19].

To conclude, phase inversion is induced by the exchange of one-phase region into a two-phase region and results in asymmetrically structured membrane formation. Phase inversion is executed by thermodynamic instability created by external influences such as the composition or temperature of the polymeric solution. The external influences that create precipitation of polymer are used to classify the phase inversion methods, including [18]:

- Thermally induced phase separation (TIPS): phase inversion is caused by temperature differences.
- Non-solvent induced phase separation (NIPS): phase inversion is caused by non-solvent exchange in polymeric solution.
- Drying induced phase separation (DIPS): phase inversion is caused by evaporation of polymeric solution components.
- Vapour induced phase separation (VIPS): phase inversion is caused by evaporation of non-solvent chemicals.

The precipitation phenomenon occurs by applying a single phase inversion technique or combining them [18]. The subsurface layer of the resulting film of phase inversion is diversified by casting solution differences, CB temperature differences, and solution additives differences [19].

2.2.2.1 Thermally Induced Phase Separation

The polymeric solution of this method is an unstably thermal polymer-solvent system, which is homogeneous at high temperatures but transforms into a two-phase system (polymer-rich phase and polymer-poor phase) at lower temperatures [18]. The solvent of polymeric solution proceeds like solvent at high temperature and non-solvent at low temperature in the phase inversion process.

2.2.2.2 Non – solvent Induced Phase Separation

In this method, a coagulation bath is fulfilled by non – solvent solution. The phenomenon of NIPS is a two-phase inversion process inducing polymer precipitation, which has been commonly applied for asymmetric membrane preparation [18].

- Polymer-rich phase (solid-liquid demixing) occurs by the gelation (crystallization) of polymeric solution (the polymer in casting solution transfer to the crystallization form, become to the semi-crystalline or crystalline polymer), and form the membrane matrix.
- Polymer-poor phase (liquid-liquid demixing) occurs by exchanging solvent of casted solution with non-solvent solution in coagulation bath and creates the porous network of the membrane.

NIPS is defined as simultaneously physical reactions [16]:

- The displacement of solvent and non-solvent by mass transfer.
- The precipitation of polymer-rich phase.
- The solidification of polymer-rich phase.

Figures 2-5 show the displacing of solvent and non-solvent in the NIPS technique while water acts like non – solvent solution [18].

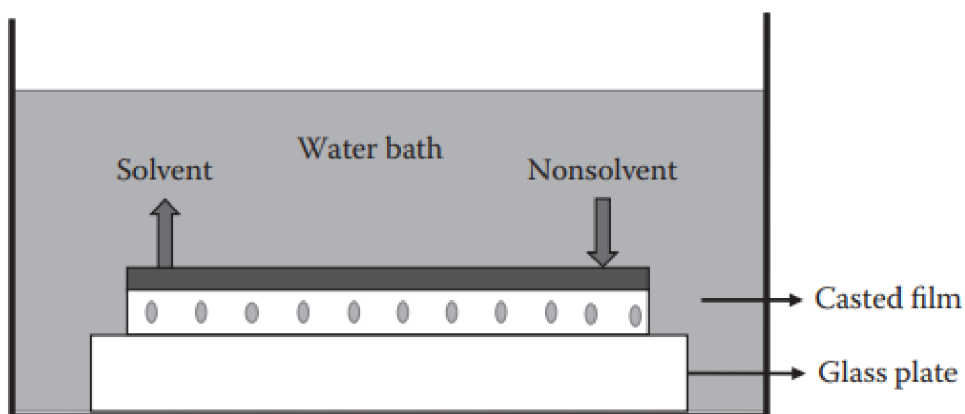


Figure 2-5 Schematic of non – solvent induced phase separation process [18].

In the ternary phase diagram of Strathmann's, the polymer precipitation rates were not described and this concept was quite oversimplified. Wijmans et al. considered this precipitation rate changed throughout the thin film thickness, resulting in asymmetric membrane structures [20]. The top layer of the casted film quickly precipitates right after immersion, it is not enough time for sublayer coarsening, bringing about tiny pores. The precipitated top layer then goes about as a barrier to the decreasing of solvent and the increasing of non-solvent for the remainder of the film. In this manner, the precipitation rate diminishes from the top layer of the film to the bottom. Due to the diminishing of the precipitation rate, pore diameter increases because of more coarsening before solidification [20].

2.2.2.3 Drying Induced Phase Separation

The polymeric solution of this method is prepared by dissolving polymer into the volatile solvent, while non-solvent is prepared by low or non-volatility chemicals. Phase separation occurs when the solvent is dried or evaporated after casting because its solubility quickly decreases. The result of the separation process is a dense polymer film by membrane precipitation [18].

2.2.2.4 Vapour Induced Phase Separation

Vapor-induced phase separation occurs when the evaporation of non-solvent saturates with casted film. VIPS method combines dry and wet casting process. First, the casted film is displayed to non-solvent vapor and then, immersed in CB for finishing the separation [18].

2.3 Polymeric solution

Various methods are possible to fabricate the microfiltration membrane such as electrospinning, phase inversion, and mechanical stretching [18,21]. Several studies show that the NIPS technique is one of the most feasible methods to prepare a MF membrane. It is also proved that NIPS can diversify pore structures, transfer high permeability, and good mechanical properties in the resulting membrane.

The properties of membrane prepared by the NIPS technique are defined by the influence of concentration and composition of casting solution, the solvent in polymeric solution, and coagulation bath temperature [22]. The asymmetric structure of the membrane in the NIPS technique is highly dependent on the casting solution and coagulation bath [18]. The different crystallization of the polymers give the resulting membrane different properties, thus, the selection of the polymer is crucial to get a membrane with desired properties [18].

2.3.1 Characteristic of PVDF as a membrane material

2.3.1.1 Crystalline property of PVDF

PVDF is a semi-crystalline polymer, widely used as a membrane material due to its superior physicochemical properties. PVDF constitutes of a $-\text{CH}_2 - \text{CF}_2 -$ repeating unit, commonly contains 3 wt% hydrogen and 59.4 wt% fluorine [23].

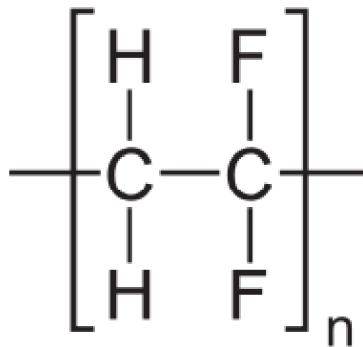


Figure 2-6 Chemical structure of PVDF

The amorphous phase of polymer offers flexible and good mechanical properties, while the crystalline phase gives thermal and chemical resistance, antifouling, anti UV radiation, and organic non-adsorption properties [24]. Hence, PVDF membrane could filter the organic particles such as carbohydrates, proteins, and fats. However, PVDF has a few disadvantages, such as its hydrophobicity, low porosity, and less functional group [25].

Despite the hydrophobicity property, there are various appropriate solvents selection for PVDF easily dissolving, as a result, it helps to enhance hydrophilicity in the resulting membrane. This is the principal reason why PVDF is still the most ideal material for membrane fabrication [26]. Hence, enhancing hydrophilicity as well as fouling resistance of PVDF membranes is a crucial issue that needs to be tackled. On this matter, the character of PVDF solution is optimized to tune the crystalline polymorphous structures by modifying solution concentration, solution composition, solution solvent, and solution additives [27].

Generally, the membrane mechanical strength and also its resistance are influenced by the polymer crystallinity [28]. PVDF crystallised chains can be obtained by at least four different forms, including α (form II), β (form I), γ (form III), δ (form IV) [29].

Membrane pore structures depends on thermodynamics and kinetics of the polymer system. While the α phase of PVDF acts as a kinetic polymorph and the β phase is thermodynamic stabilization [27]. Hence, the α and β form are the most well-known crystalline structures in PVDF membrane produced by NIPS method [27].

In the α -PVDF phase, the trans-gauche (TGTG') chains are conformed by H and F atoms deposited in alternate directions, and become non-polar chain [27]. When PVDF membrane overwhelmed by the non-polar chain, the reactions between the surface layer and polarized water particles are low-powered. Subsequently, the α -PVDF phase lets the contaminants easily deposit on the membrane surface by hydrophobic interaction [27].

The β -PVDF phase can be produced from the α -PVDF phase by different methods, such as “mechanical deformation, poling under large electric fields, and crystallization from the melt under

high pressure or very high cooling rates” [30]. In the β -PVDF phase, the planar zigzag (TTTT) chains are conformed. The particular polarizations of the polymer chains are arrayed in the same direction and make it become a nonzero net dipole moment and the strongest polarized chain among all four different PVDF phases [27]. Therefore, the β -PVDF membrane is considered to have a stronger interaction with polarized particles than other phases by the rule of Polar Spreads on Polar [31], and those surface interactions help to enhance the membrane anti-fouling property [27].

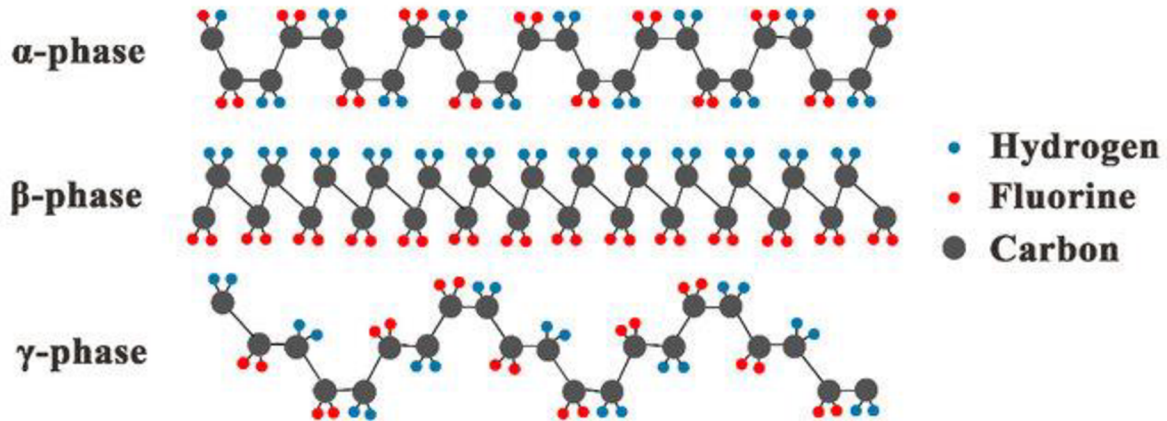


Figure 2-7 Structures of α , β , and γ PVDF phase [32].

Fane et al. introduced a formula to calculate the PVDF crystallinity [33]. The 10mg polymer test specimens were heated from room temperature up to 180 °C at 10 °C/min. The degree of crystallinity of membranes was determined by the below formula:

$$\chi_c = \frac{\Delta H}{\Delta H_m} \times 100\%$$

- χ_c denotes the degree of crystallinity (in %)
- ΔH denotes the melting enthalpy of membrane (in Joule/gram)
- $\Delta H_m = 104.5$ (Joule/gram) denotes the melting enthalpy of 100% crystallinity PVDF

The crystalline polymorphous structures are also adjusted by different types of polymers, such as substrates, copolymers, and blending polymers [22]. Using blending polymers is a popular method to control the porous system and hydrophilicity of the PVDF membranes. The primary drawback of PVDF blending polymer is that additives in the solution are progressively washed out. Due to the washout of additive, the pore diameter is essentially amplified and the membrane selectivity is weakened. Moreover, the increase of surface hydrophobicity diminishes membrane fouling resistance as well as membrane stability [27].

2.3.1.2 Thermal stability property of PVDF

PVDF overwhelms other types of polymer in thermal stability due to its C–F bond group. Generally, fluoropolymers are higher thermally stability than hydrocarbon polymers, this phenomenon is provided by the high electronegativity of fluorine atoms on the chain and the high bond dissociation energy of the C–F bond [34].

Furusho et al. introduced that PVDF was one of the most thermally stable polymers using halogen compounds by Torsional Braid Analysis (TBA) method. PVDF ultrafiltration membrane was prepared by commercial Kynar polymer, and determined the thermal stability property by spiral-wound modules. The prepared PVDF membrane had been under 85.6 °C temperature and constant pressure for seven months. It was proved that thermal degradation of PVDF membrane experienced fairly unchanged. In this study, the thermogravimetric analysis (TGA) of six different polymers was also investigated. The weight loss led by the dehydrochlorination reaction of PVDF started at about 350°C and became intense between 380°C and 430°C, and was one of the most stable material compared with other polymers [35].

Figure 2-8 illustrated the TGA of six different polymers in Furusho's study, each number represented for one type of investigated polymer.

- (1) Polyvinylidene bromide (PVDB).
- (2) Polyvinyl bromide (PVB).
- (3) Vinylidene chloride - vinyl chloride copolymer (PVDC-VC).
- (4) Polyvinyl chloride (PVC).
- (5) Polyvinyl fluoride (PVF).
- (6) PVDF.

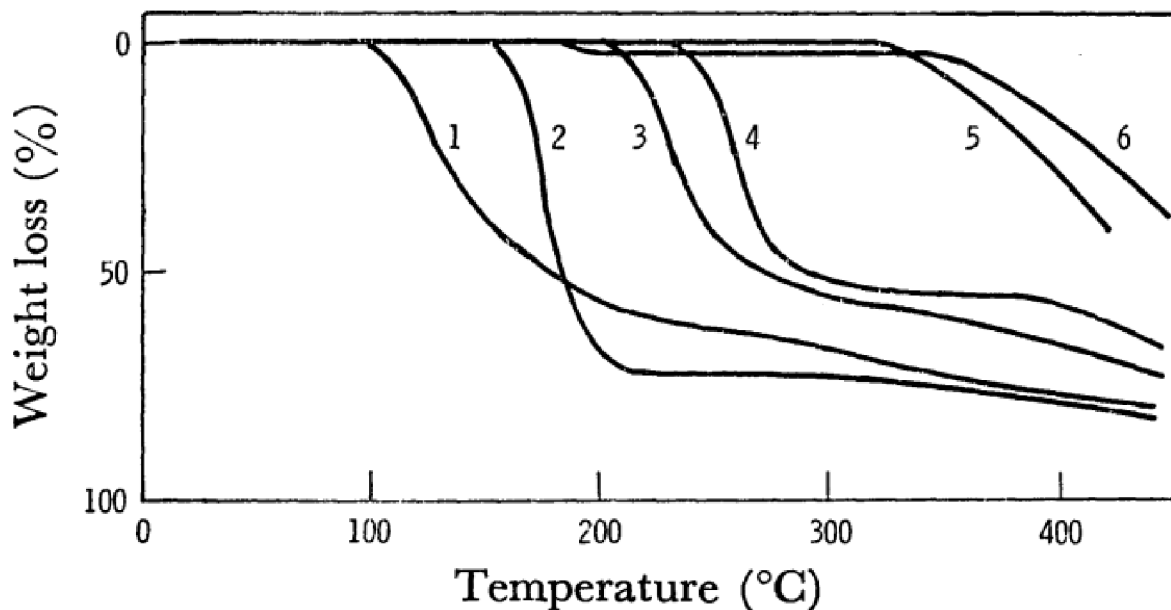


Figure 2-8 TGA thermograms of halogen-containing polymers in air [35].

Hashim introduced the comparison of thermal stabilities between PVDF with other polymers frequently used in commercial membrane industry, including: polypropylene (PP), polyethylene (PE), polytetrafluoroethylene (PTFE), polysulfone (PS), polyethersulfone (PES) and polyimide (PI). It shown the stable of PVDF with thermal resistance compared with other six popular polymers [36], the information was listed in table 2-2.

Table 2-2 Thermal stability of frequently used polymer in membrane industry [36].

Thermal stability	PVDF	PP	PE	PTFE	PS	PES	PI
Melting point (in °C)	140 – 170	130 – 170	118 – 146	310 – 385		340 – 390	350 – 390
Glass transition temperature (in °C)	-41 / -38	2 / 10	-118 / -127		185	225	120 / 370
Thermal stability 1% mass loss in air (in °C)	375					400	
Linear thermal expansion coefficient (in $10^{-6}/^{\circ}\text{C}$)	50 – 103 or 120 – 140	140 – 180		14 – 250	28.8 – 103	55	55

However, PVDF experiences thermally unstable under certain harsh operations. PVDF thermal decomposition occurs at moderate and high temperatures in vacuum [37], or ambient temperature surpasses 375°C [38], and charring circumstance occurs when material weight loss is up to 70% [38]. The pyrolysis mechanism is dehydrofluorination in PVDF polymer chain and releasing

hydrogen fluoride (HF) gas. It subsequently prompts to several chemical reactions, mainly including carbon-carbon double bonds formation (-C=C-) and the cross-linking of the polymer under cumulative temperature conditions [37,38]. Meanwhile, PVDF inhomogeneous thermal degradation phenomenon at was investigated by Lovinger and Freed in 1980. The pyrolysis is majority in crystalline segments while amorphous segments remain unchanged, and this extraordinary circumstance cannot be observed in other polymers [39].

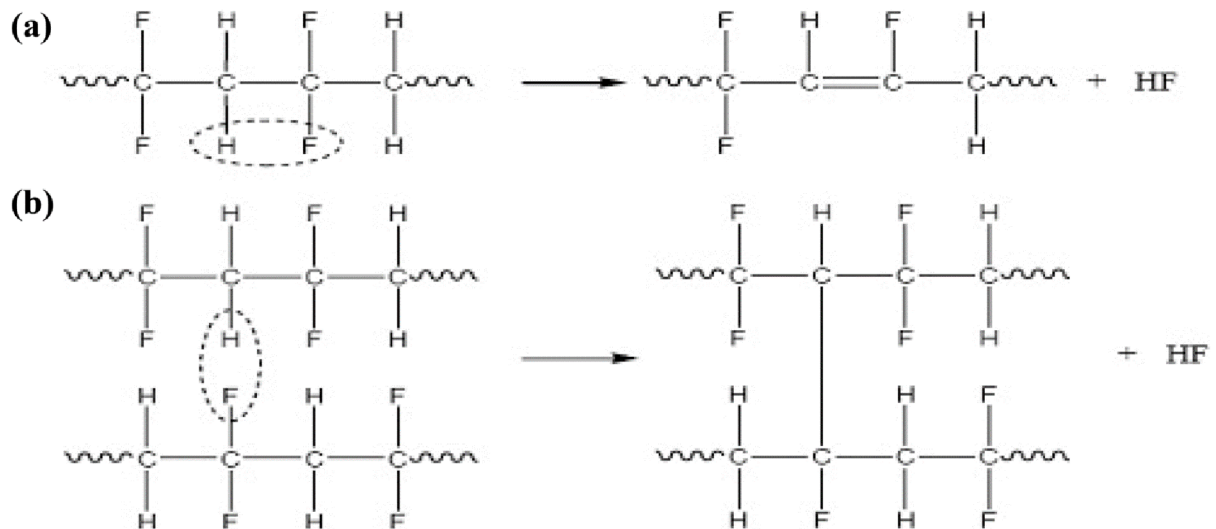


Figure 2-9 Dehydrofluorination reaction in PVDF by (a) formation of double bond and (b) cross-linking of polymer [37].

2.3.1.3 Chemical resistance property of PVDF

PVDF demonstrate the advantages in chemical stability against a wide range of harsh chemicals, including oxidants, halogens, inorganic acids, aliphatic, aromatic and chlorinated solvents [2,29,36]. However, the outstanding chemical resistance of PVDF does not maintain well in caustic medium, such as strong base solutions or in esters and ketoneset. The chemical stability of PVDF membranes, especially in water filtration, can be influenced by many elements, including the exposed time, substance concentrations, treatment temperature, treatment pressure, frequency of the attack cycles.

It raises a particular concern in contactor membrane application since strongly alkaline solution is imposed on PVDF membrane during filtration, and consequently creates chemical instability of membrane [40].

The PVDF chemical degradation created by alkaline solutions was examined by Shinohara's study in 1979. The color of PVDF thin film immersed in alkaline solution after few hours was changed from white to brown and black in the end. This discolouration of oxyfluorinated PVDF film occurs simultaneously with the dehydrofluorination causing the carbon-carbon double bonds formation

in PVDF polymer chain [40]. Despite the chemical resistance to harsh chemicals, PVDF stability is strongly effected by concentrated sodium hydroxide (NaOH) solution. The performance of PVDF membrane exposed by NaOH solution is significantly decreased, comparing with wool scouring wastewater, acids, calcium chloride and sodium bisulfite solution [41].

2.3.2 Characteristic of DMAc as polymeric solvent

The auxiliaries are substances that do not directly influence to the chemical structure of the final materials, also, are required for the ideal process reaction. In membrane formation via NIPS method, solvents act as the primary auxiliaries, is utilized for dissolving the chosen polymer and is displaced by non-solvent, consequently create porous system [42].

N,N-Dimethylacetamide (DMAc) is an organic compound and utilized as traditional petroleum-based solvents. It is widely used in membrane synthesis due to its dissolubility with most of polymeric materials including PVDF and its miscibility with other solvents [43].

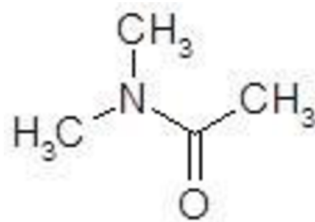


Figure 2-10 Chemical structure of DMAc.

The combination of PVDF with DMAc is more remarkable due to its ease to dissolve compared with others, including tetraethyl phosphate (TEP), N-methyl-2-pyrrolidone (NMP), and dimethylformamide (DMF). DMAc is a polar solvent, the polarized character empowers it to work as a dissolvable solvent and reaction catalyst in numerous chemical reactions. This supports to high productivity reactions and pure yields of reactions products in short time periods. DMAc is also a good polymer dissolution because of its high boiling point and high thermal and chemical resistance [43].

Figure 2-11 shows the dissolvable solvent exchanges with non-solvent to create porous system during membrane formation by NIPS method.

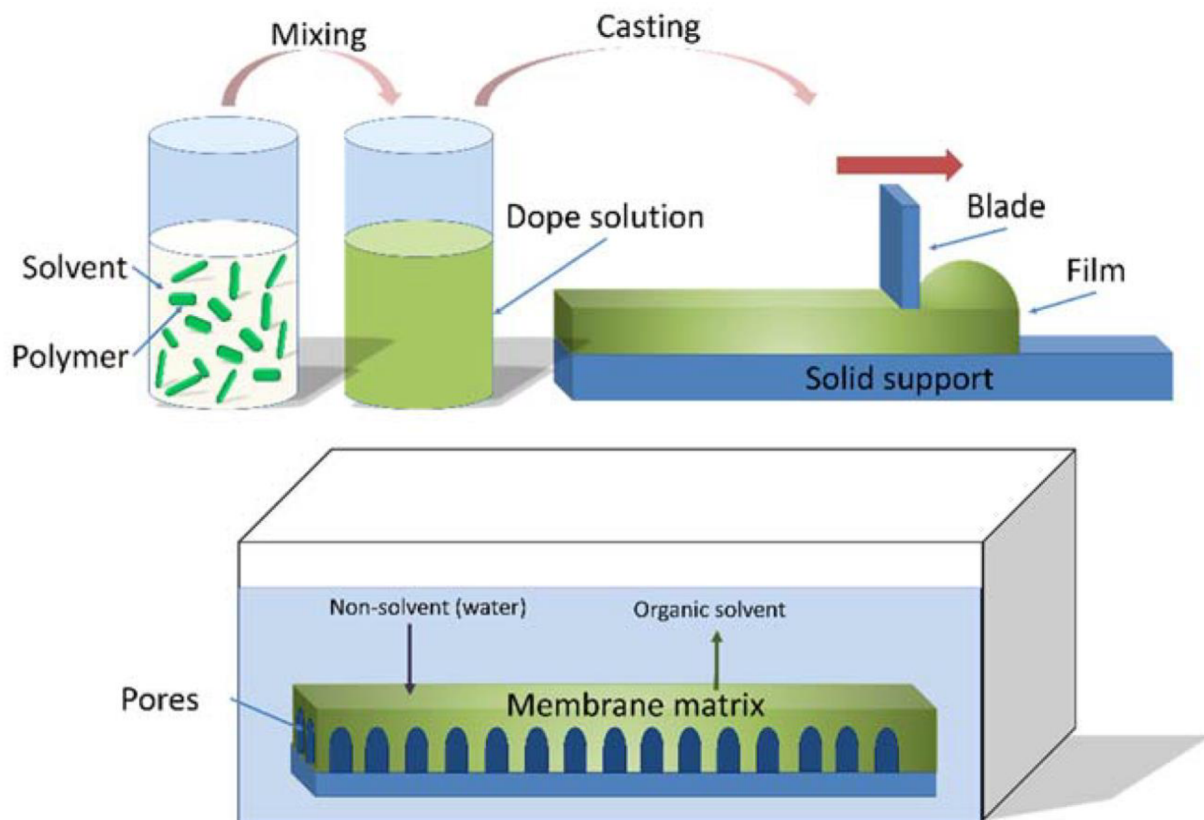


Figure 2-11 Non-solvent phase inversion casting process [12].

Conventional solvents utilized for membrane synthesis such as DMAc, DMSO, TEP, NMP, and DMF can cause negative impacts to environment and human health after exposure. Some of these solvents are hazardous substance, for example, “DMAc, and DMSO are mutagenic and tumorigenic; acetone is highly flammable; and NMP is an irritant. Acute effects of DMF include skin irritation and dizziness, while its long-term effects are known to cause birth defects” [12].

2.3.3 Characteristic of polymeric additives

In NIPS method, the membrane formation is defined by the phase inversion route and rate. Meanwhile, the phase inversion are consequently influenced by dope solution composition and the precipitation conditions (including coagulation composition, coagulation bath temperature, ambient conditions, and so on), because both parameters can influence to the thermodynamics and kinetics of polymer system [18].

Moreover, polymer and polymeric additives, and solvent and non-solvent can be utilized to modify the dope solution character and subsequently to adjust the membrane formation process. Using additives is a common and powerful method to modify the dope solution, therefore it can consequently adjust the membrane structure and properties to achieve a high performance membrane. A variety of additives have been proposed, including macromolecular and

micromolecular polymeric additives, organic acids, inorganic acid or salts, strong non-solvent additive, and blended additives [18].

The most two commonly used additives for PVDF dope solution are polyvinylpyrrolidone (PVP) and polyethylene glycol (PEG). The impact of altering concentrations and molecular weights of PVP and PEG on membrane structure and performance were studied in numerous researches. The investigations aim to comprehend their influence on the membrane synthesis process [2,14,44].

Using PVP or PEG as additives for dope solution, which has the hydrophobic characteristic, during membrane formation, is to increase the hydrophilic of membrane surface. It also can effect to the viscosity of dope solution, hence, effect to the diffusive exchange rate during phase inversion process. Following that, it impacts to the resulting porous system of membrane, including the pore sizes and macrovoids formation [44]. In asymmetric membrane, macrovoid structure is large and elongated pores that diminish the mechanical resistance as well as separation performance of membrane [16].

The porous system of membrane depends on the adjustment of coalescence of the polymer-poor phase and accordingly on the change of the sizes of the remaining holes inside the membrane matrix when the viscosity is modified. Moreover, PVP and PEG are assigned as pore-forming chemicals due to their impact to membrane fluid stream and permeability, as well as the membrane structure and its stability in many investigated studies [2,14,44].

2.3.3.1 Characteristic of PVP as a polymeric additive

PVP is a non-toxic, non-ionic amorphous polymer with high solubility in polar solvents, widely used as a membrane-forming additive [45].

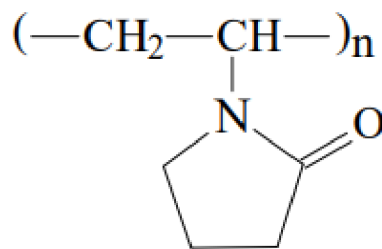


Figure 2-12 Chemical structure of PVP [45].

PVP is a miscible and amphiphilic polymer, its molecule contains an pyrrolidine compound, lead to its strong hydrophilic property, and an alkyl group, act as a hydrophobic part. The polarization of PVP is given by polarized amide group in pyrrolidine ring and apolarized methylene and methane groups in pyrrolidine ring and in backbone chain [46]. Therefore PVP enables to dissolve in different solvents [45].

PVP can act as surface stabilizer to prevent the agglomeration of particles in polymeric solution via the repulsive forces. The repulsive forces are arisen from its hydrophobic carbon chains interacting with each other in a solvent (Steric hindrance effect) [46].

Adding PVP can enhance the hydrophilicity of final polymer system, lead to the membrane surface modifications as well as membrane porous system, and increase membrane filtration execution. However, the membrane surface modifications could reduce the membrane pore sizes and membrane fluid flux because PVP is swelled up and stuck into membrane pore walls [45].

Many studies show that PVDF is well miscible with PVP, creates a good mechanical resistance membrane with high porosity channel [47]. The pore size of porous system should be controlled under $0.1\mu\text{m}$ to balance the membrane permeation and rejection rate [5,8,47].

PVP is well known as a perspective additive with good pore-forming ability, therefore it is expected that PVP helps to enhance the hydrophilicity and the desirable filtration performance of the casting PVDF membrane.

2.3.3.2 Characteristic of PEG as a polymeric additive

PEG is a hydrophilic, non-toxic, flexible and non-volatile polyether compound with incredible solubility in water and organic solvents, and widely used as a membrane-forming additive [48].

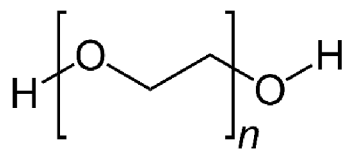


Figure 2-13 Chemical structure of PEG [48].

PEG is a miscible and amphiphilic polymer, normally produced by opening ethylene oxide ring to form the ethylene glycol. Its molecule contains repeating units of ethylene oxide with terminal hydroxyl group, lead to its strong hydrophilic property, and the $-\text{CH}_2 - \text{CH}_2 -$ group act as a hydrophobic part [48].

PEG is suitable in numerous applications, its molecular weight is varied from 200 g/mol to 10,000,000 g/mol, offers variety of properties due to different polymer chain length effect [48].

PEG has extremely high aqueous solubility, especially PEG polymer with $n \leq 600$ is infinitely soluble in water. Its solubility is not a direct result of Steric effect, but because “the partial charge on the oxygen atoms depends on the number of carbon atoms by which they are separated” [49].

The addition of PEG to PVDF solution let the active OH group enter to PVDF backbone chain, results in better diffusion of non-solvent into the membrane. Therefore, it was proved that adding PEG to polymer system could enhance the porosity, hydrophilicity, and filtration performance of

resulting PVDF membrane. The membrane mechanical strength was also improved due to decreasing finger-like voids formation [50,51].

2.4 Membranes preparation

PVDF is well known as hydrophobic nature and contain an adequate number of functional imide groups that can be functionalized [2]. Recently, microporous membranes formed by PVDF-based copolymers become popular due to its higher hydrophilicity, better mechanical, thermal, and chemical resistance.

The NIPS method requires reasonable expense for the membrane matrix modification, along with sufficiently hydrophilic property.

Aside from the process conditions, the composition of the polymeric solution involves a significant effect on the thermodynamics and kinetics of the membrane formation, strongly impact to membrane properties.

Because the membrane formation relies upon various unpredictable factors due to the interaction and combination of each membrane formation condition, therefore, there is still an extraordinary demand to explore the better understanding of mechanism of membrane formation.

In this study, different membranes were fabricated by using NIPS technique with PVDF casting solution and NaCl coagulation bath. The NaCl coagulation bath were used to make ion-dipole interactions among Na⁺ and PVDF, this boosts the β -PVDF phase formation (which is the strongest polarized form of PVDF) during phase inversion process [52]. It was supposed to enhance antifouling ability of fabricated membranes.

It was expected to create porous membrane with high permeability and good mechanical properties. A series of PVDF membranes with PVP and PEG acting as additives were prepared and investigated. The membrane structures and properties were examined in the manner of various compositions. Finally, the impacts of the various factors on the membrane performance in terms of permeability, rejection rate, and surface characteristics were evaluated.

3 Materials, Apparatus, and Procedures

3.1 Characteristics of used chemicals

To study the characteristics of microporous PVDF membranes in different hydrophilic additives systems (PEG and PVP), membranes with varying concentrations of PVDF, PVP, and PEG were prepared.

PVDF powder (density $\rho = 1.78 \text{ g/cm}^3$) was chosen as the polymer material, supplied by Arkema.

N,N-Dimethylacetamide (DMAc) (molar mass $M = 87,12 \text{ g/mol}$, $\rho = 0,937 \text{ g/cm}^3$ at 25°C) was used as the solvent in membrane preparation and provided by Penta Chemicals Unlimited.

While PEG (average molecular weight $M_n = 400 \text{ g/mol}$, $\rho = 1.128 \text{ g/cm}^3$ at 25°C), PVP powder ($M_n = 40,000 \text{ g/mol}$) was added as non-solvent additives, purchased from Sigma Aldrich, Germany.

Sodium chloride (NaCl, $M = 58,44 \text{ g/mol}$), used for the coagulation bath, and Glycerol anhydrous (Glycerin, $M = 92,1 \text{ g/mol}$, $\rho = 1,258 - 1,263 \text{ g/cm}^3$ at 20°C), used for maintaining membrane pore size, were acquired from Penta Chemicals s.r.o.

3.2 Polymeric solution preparation

The polymeric solution was prepared by mixing PVDF powder (in three different contents: 10%, 15%, and 20%) in DMAc solvent. Then, PVP or PEG additives would be added into polymer-solvent mixtures at various concentrations (2%, 5%, and 8%). 21 different solutions were produced totally and the compositions of the polymer solutions were shown in Table 3-1.

Table 3-1 Composition of the polymeric solution.

Sample No.	Polymeric solution	Polymeric concentration (w/v %)	Sample abbreviation
1	10g PVDF in 100ml DMAc	PVDF 10%	PVDF - 10
2	2g PVP in 100ml PVDF 10%	PVP 2% / PVDF 10%	PVDF - 10 / PVP 2
3	5g PVP in 100ml PVDF 10%	PVP 5% / PVDF 10%	PVDF - 10 / PVP 5
4	8g PVP in 100ml PVDF 10%	PVP 8% / PVDF 10%	PVDF - 10 / PVP 8
5	2g PEG in 100ml PVDF 10%	PEG 2% / PVDF 10%	PVDF - 10 / PEG 2
6	5g PEG in 100ml PVDF 10%	PEG 5% / PVDF 10%	PVDF - 10 / PEG 5
7	8g PEG in 100ml PVDF 10%	PEG 8% / PVDF 10%	PVDF - 10 / PEG 8
8	15g PVDF in 100ml DMAc	PVDF 15%	PVDF - 15
9	2g PVP in 100ml PVDF 15%	PVP 2% / PVDF 15%	PVDF - 15 / PVP 2
10	5g PVP in 100ml PVDF 15%	PVP 5% / PVDF 15%	PVDF - 15 / PVP 5
11	8g PVP in 100ml PVDF 15%	PVP 8% / PVDF 15%	PVDF - 15 / PVP 8

12	2g PEG in 100ml PVDF 15%	PEG 2% / PVDF 15%	PVDF - 15 / PEG 2
13	5g PEG in 100ml PVDF 15%	PEG 5% / PVDF 15%	PVDF - 15 / PEG 5
14	8g PEG in 100ml PVDF 15%	PEG 8% / PVDF 15%	PVDF - 15 / PEG 8
15	20g PVDF in 100ml DMAc	PVDF 20%	PVDF - 20
16	2g PVP in 100ml PVDF 20%	PVP 2% / PVDF 20%	PVDF - 20 / PVP 2
17	5g PVP in 100ml PVDF 20%	PVP 5% / PVDF 20%	PVDF - 20 / PVP 5
18	8g PVP in 100ml PVDF 20%	PVP 8% / PVDF 20%	PVDF - 20 / PVP 8
19	2g PEG in 100ml PVDF 20%	PEG 2% / PVDF 20%	PVDF - 20 / PEG 2
20	5g PEG in 100ml PVDF 20%	PEG 5% / PVDF 20%	PVDF - 20 / PEG 5
21	8g PEG in 100ml PVDF 20%	PEG 8% / PVDF 20%	PVDF - 20 / PEG 8

The solution was heated to approximately 60°C and magnetically stirred at 400 rpm by Magnetic Stirrer from Heidolph company until the polymer and additives were completely dissolved. The results were viscous and homogeneous polymeric solutions. Those solutions, called the casting solutions or dope solutions, were degassed overnight to remove any visible gas bubbles present in the solution. After degassing, the formed solutions were ready to be cast into the thin films.

3.3 Membrane preparation by NIPS technique

The flat sheet membrane was fabricated by NIPS technique, by various polymeric solutions with DMAc as a solvent and NaCl solution as a non-solvent. The following steps were described how the flat sheet membranes were produced on laboratory – scale.

- After degassing, the dope solution was spread onto the glass plate and manually cast by a casting blade (VF1502-448 – TQC sheen) in a fixed thickness of 200 µm.
- The glass plate containing a thin layer of dope solution was immediately immersed in sodium chloride CB for phase inversion. The bath was filled with 5 wt% NaCl (non-solvent) in water and maintained at room temperature. The glass plate was left in the bath for 5 minutes to completely exchange solvent and non-solvent, which resulted in asymmetric microstructure membranes.
- After the thin polymeric film was solidified and separated from the glass, they were taken from CB and followed by a thorough rinse with DI water to remove the traces of solvent. After fabrication, membranes were impregnated in 40 wt% glycerin solution overnight. Glycerin post-treatment was applied to fill the membrane pores and protect them from shrinkage or collapsing of pore structure during storage before membrane characterization. Membranes were then dried in an oven for 2 hours at 60°C to remove the excess non-solvent in the membrane matrix. All samples were stored in plastic zip bags until further membrane characterization.
- Before the characterized, the membranes were just flushed with distilled water for getting rid of glycerin.

The NIPS process on laboratory – scale is sketched in Figure 3-1, which is described below [53]:

- a) Casting the dope solution on a glass plate by casting blade.
- b) Phase inversion by immersion cast film in the coagulation bath.

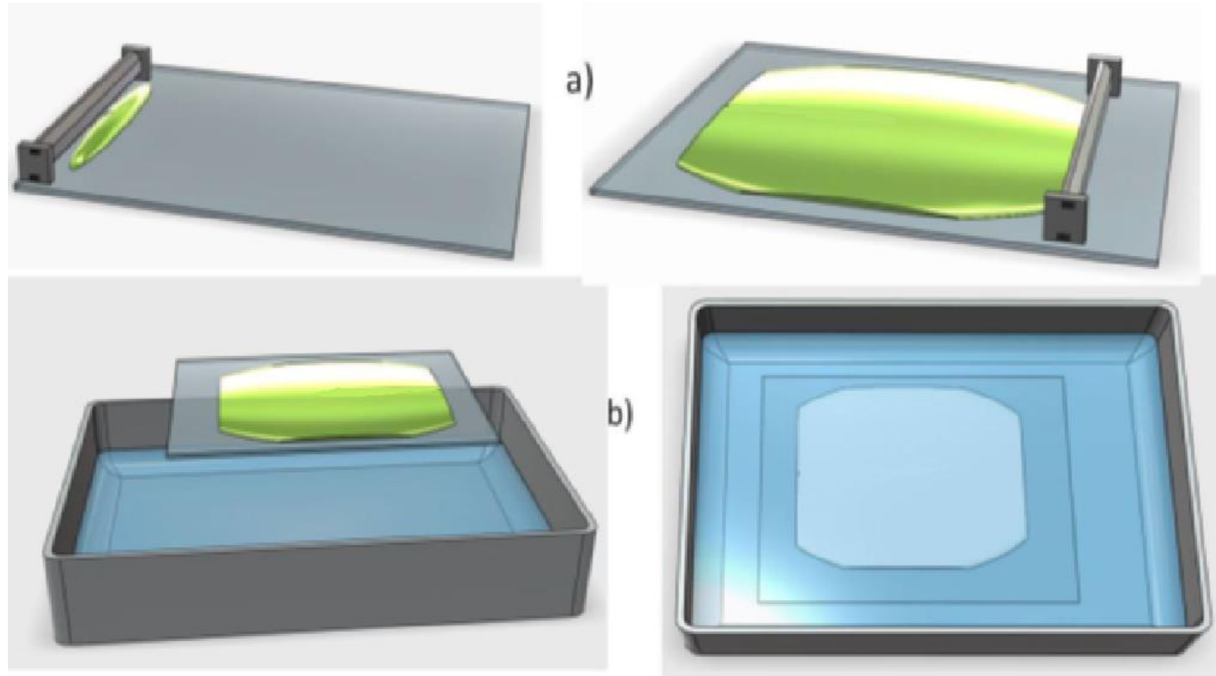


Figure 3-1 Schematic of NIPS process on lab – scale.

3.4 Membrane characterization

The phase separation made numerous changes in the physical and chemical properties of fabricated membranes. Different characterization methods were applied to investigate membrane properties, such as water contact angle, membrane filtration performance, water uptake and swelling degree of membrane. ImageJ software analyzed scanning electron microscope (SEM, Tecan Vega3) images of membranes to determine their microstructure, such as membrane thickness and average membrane pore diameter. Besides, Fourier transform infrared spectroscopy (FTIR – Nicolet iZ10) analysis defined chemical compositions in membranes. Meanwhile, the filtration performance of the selected casting membranes was also obtained in the micropollutant separation experiment.

3.4.1 Fourier transform infrared spectroscopy

Fourier Transform Infrared Spectroscopy (FTIR) is typical qualitative analysis to define functional group on surface of membrane [5]. It measures by a broad spectrum in the infrared radiation that is absorbed by a test specimen. The chemical properties of the membranes were investigated by using FTIR [54].

For the measurement, a thin sheet of membrane was placed in the sample holder. The FTIR spectra were obtained in the wavelength range of 4000 to 400 cm^{-1} for gas analysis by using Nicolet iZ10 from Thermo Scientific, USA.

The FTIR analysis result was utilized to examine the occurrence of chemical compositions of PVP and PEG additive in PVDF membrane.

3.4.2 Membrane pore diameter and membrane thickness

The surface morphology and cross-section of the membranes was investigated using a scanning electron microscope (SEM) image. In this study, Tescan Vega3 instrument from Tescan Orsay Holding, a.s was used to capture SEM image.

The specimens were sputter coated with a thin layer of gold under vacuum, then were captured SEM image by instrument with an acceleration voltage of 30 kV. The recorded images were utilized for statistical analysis by ImageJ software (National Institutes of Health, USA). The surface images were used to determine membrane pore diameter while the cross-section determined membrane thickness.

For each membrane, the pore size was taken by highest probability bin value in histogram chart of each membrane pore measurement data. The membrane thickness was measured and averaged by at least five different regions.

3.4.3 Contact angle

The contact angle is a typical measurement to evaluate the hydrophilicity of the membrane surface. The angle is formed between the membrane surface and a tangent to the curved surface of the liquid droplet [55]. The wettability of the membrane varies inversely with the contact angle value, which is smaller contact angle, higher wettability [55,56].

Young introduced the measurement of the equilibrium contact angle on a non-textured or smooth surface, it applied for any dropping liquid and demonstrated as below formula [55,56]:

$$\cos \theta = \frac{\gamma_{sv} - \gamma_{sl}}{\gamma_{lv}}$$

- θ (unit in degree) denoted for the equilibrium contact angle.
- S, l, v denoted for solid, liquid and vapour phase respectively.
- γ (unit in milli-Newtons per meter, mN/m) denoted for the interfacial tension, where γ_{sv} is the solid-vapour interfacial tension (referred as the solid surface energy), γ_{sl} is the solid-liquid interfacial tension, γ_{lv} is the liquid-vapour interfacial tension (referred as the liquid surface tension).

The figure below shows the schematic of a sessile-drop contact angle system where θ_Y is Young's contact angle.

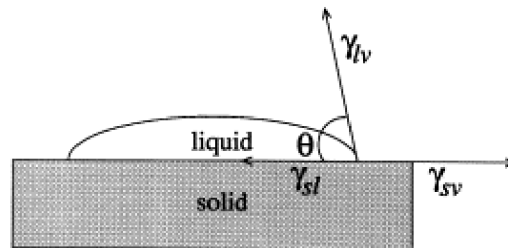


Figure 3-2 Schematic of a sessile-drop contact angle system [55].

A surface can be classified its wetting ability based on the value of contact angle [56]:

- Superhydrophilic when $\theta \approx 0^\circ$.
- Hydrophilic when $\theta < 90^\circ$.
- Hydrophobic when $\theta > 90^\circ$.
- Superhydrophobic when $\theta > 150^\circ$ and the contact angle hysteresis is below 5° .

The contact angle hysteresis is measured by the difference between the advancing contact angle and the receding contact angle on a substrate surface. The advancing contact angle is measured when the contact line between the surface and droplet is increasing. The receding contact angle is measured when the contact line between the surface and droplet is withdrawing [57].

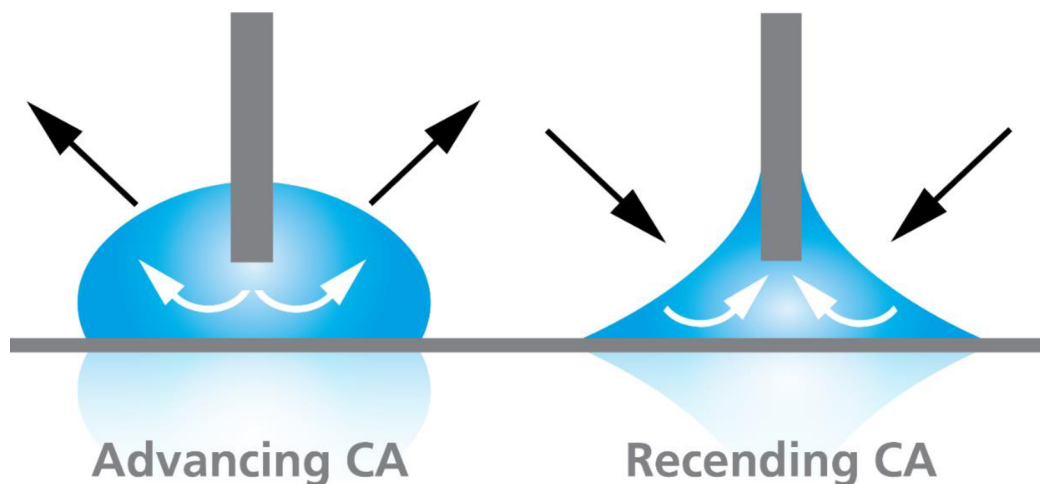


Figure 3-3 The advancing and the receding contact angle [57].

Figure 3-4 shows the contact angle of different surface substrates with water droplet [56].

- a) Superhydrophilic surface with $\theta = 3^\circ$.

- b) Hydrophilic surface with $\theta = 20^\circ$.
- c) Hydrophobic surface with $\theta = 118^\circ$.
- d) Superhydrophobic surface with $\theta = 155^\circ$ and very low contact angle hysteresis.

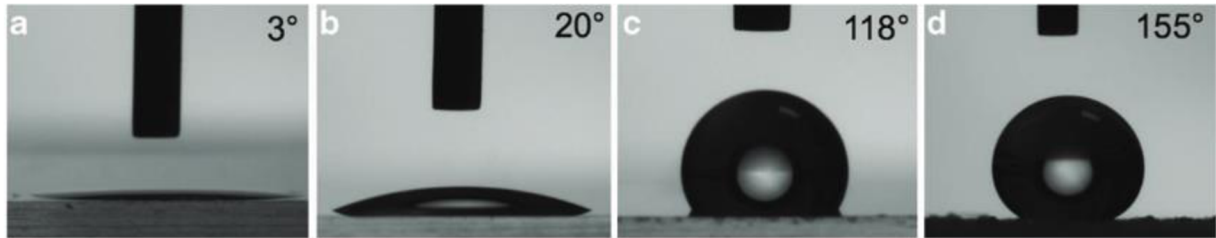


Figure 3-4 Surface wetting ability classification by contact angle [56].

The membrane water contact angle was directly measured by the sessile drop method. This method illustrates the wetting ability of a membrane surface when liquid was applied to its surface [55].

For the measurement, a deionized water droplet was dripped to a dry membrane surface through a fine tip by using Drop Shape Analyzer DSA30E from KRÜSS GmbH for the liquid dispensed controller. The droplet image was visualized by DSA4 – Drop Shape Analysis software to analyse the water contact angle.

The final result of the contact angle was the mean value of the right and left angle calculation using the image analysis software.

3.4.4 Water uptake and swelling degree of membrane

Membrane water uptake measurement is obtained by weight changing after membrane is swollen in deionized water. The water uptake demonstrates the water adsorption ability of membrane which is a crucial characteristic in filtration technology [58,59]. Moreover, the water absorption is used to define the hydrophilicity of the membrane and directly related to membrane porosity [59].

The higher water uptake according to higher inner space free volume in material is better for water transportation, which is better for filtration performance [60].

Meanwhile, the swelling degree measurement is a comparison the dimensions between the hydrated membrane by immersing in deionized water and the dried membrane. The diminished swelling ratio increases the rigidity of voids formation in membrane matrix, leading to better membrane stability [60].

The swelling degree varies inversely with the membrane stability, which is lower swelling degree, higher membrane stability [60].

Firstly, the mass and dimension of dry forms were recorded after putting the membranes in oven at 80°C in 1 hour. Following that, the dried membranes were immersed in DI water in 24 hours

for full saturation. After 24 hours, the hydrated membranes were removed from DI water while the excess water on the surface of all samples were quickly removed by using absorbent paper, and then the mass and dimension of wet forms were recorded. In this study, the area of specimen was used for the swelling degree calculation. The water uptake and swelling degree are calculated as below formulas [58,60]:

$$WU (\%) = \frac{w_{wet} - w_{dry}}{w_{dry}} \times 100\%$$

- WU (unit in percentage) denoted for the water uptake value.
- w_{wet} , w_{dry} (unit in gram or milligram) denoted for the weight of wet and dry membrane samples respectively.

$$SD (\%) = \frac{a_{wet} - a_{dry}}{a_{dry}} \times 100\%$$

- SD (unit in percentage) denoted for the swelling degree value.
- a_{wet} , a_{dry} (unit in squared centimeters) denoted for the area of hydrated and dry membrane samples respectively.

3.4.5 Filtration test

3.4.5.1 Preparation of feed solution with microplastics

The polystyrene microspheres were chosen as the polybead, supplied by Polysciences Inc. The feed solutions with microplastics substance were prepared by mixing DI water with polybead, the different polystyrene microspheres sizes (0.1µm, 0.2 µm, and 0.5 µm) were used for various feed solutions.

The solutions were magnetically stirred at 400 rpm by Magnetic Stirrer from Heidolph company until the polybead was completely suspended in the water. The results were homogeneous feed solutions, which were ready for filtration test. 3 different solutions were produced and named as table 3-2.

Table 3-2 Components of the feed solution.

Feed solution	Solution components
0.1µm pollutant solution	DI water with 0.1µm mean polystyrene microspheres sizes
0.2µm pollutant solution	DI water with 0.2µm mean polystyrene microspheres sizes
0.5µm pollutant solution	DI water with 0.5µm mean polystyrene microspheres sizes

3.4.5.2 Turbidity

Turbidity is a measure for drinking water quality and its physical property is defined by the transparency of the water [61]. The clarified water becomes turbid is directly related to how much

particles in suspension as well as the particles mean size [62]. The suspended particles could be “clay and silt particles, organic matter, microscopic organisms, and colloids” [61].

Turbidity is quick and low-priced method to distinguish the presence of particles in liquid [62]. Turbidity is the optical measurement by light-scattering characteristic of a liquid sample, and measured by nephelometric turbidity units (NTUs) [61,62]. 1 NTU turbidity of the examined liquid is equivalent to 1mg of fine silica (SiO_2) per liter of water.

The turbidity typically varies from 0 to 1000 NTUs with tolerance from 2% to 3% [61], which is higher turbidity value, higher particle concentration in liquid and higher contaminated rate of the liquid.

Turbidimetry is dependent on the instruments that proceed the test, there are 4 typical instruments for turbidity measurement [63]:

- Spectrophotometer
- Jackson Candle Turbidimeter
- Secchi Disk
- Nephelometry

The most common measurement is nephelometry which uses photoelectric detectors to readout the intensity of transmitted light. The transmitted light is scattered at the right angles to the path of incident beam, the turbidity is converted from the ratio between these intensity values [63].

Turbidity measurements are significantly sensitive with “debris, settling sediments, air bubbles” in liquid as well as the cuvette cleanliness, those factors could cause an inaccurate turbidity reading [61].

In this study, the turbidity was measured by Turbidimeter TB300 IR model from Lovibond. The inspected solutions were filled into a cuvette, placed into the measuring chamber, and the turbidity values were readout in NTUs by turbidimeter device.



Figure 3-5 Turbidimeter TB300 IR model.

The table 3-3 shows the turbidity of DI water used to make pollutant solutions and 3 feed solutions prepared by polystyrene microspheres.

Table 3-3 Turbidity of DI water and feed solution.

Feed solution	Turbidity
DI water	0.91
0.1 μ m pollutant solution	10.9
0.2 μ m pollutant solution	86.9
0.5 μ m pollutant solution	58.9

3.4.5.3 Amicon dead-end filtration unit

The filtration experiments including membrane permeability and particle rejection rate were performed by using Amicon dead-end filtration (Amicon stirred cell model 8050, 50ml, UFSC05001).

In those measurements, the circular membranes with a diameter of 4.45 cm were cut and rinsed carefully with DI water before installing to Amicon dead-end filtration. The Amicon cell was filled with 40 ml filtering solutions (DI water or prepared feed solution with microplastic), while the Amicon lid was connected with pressure supply. The pressure was set to 0.25 Bar, increased stepwise up to 5 Bar if the permeability measurements could not be performed after every 3 minutes waiting period.

By this setup, the filtering solutions were filtered effectively through 13.4 cm² filtration area of circular membranes, and the time to collect 10 ml, 20 ml, 30 ml, 35 ml permeated solution in container were noted.

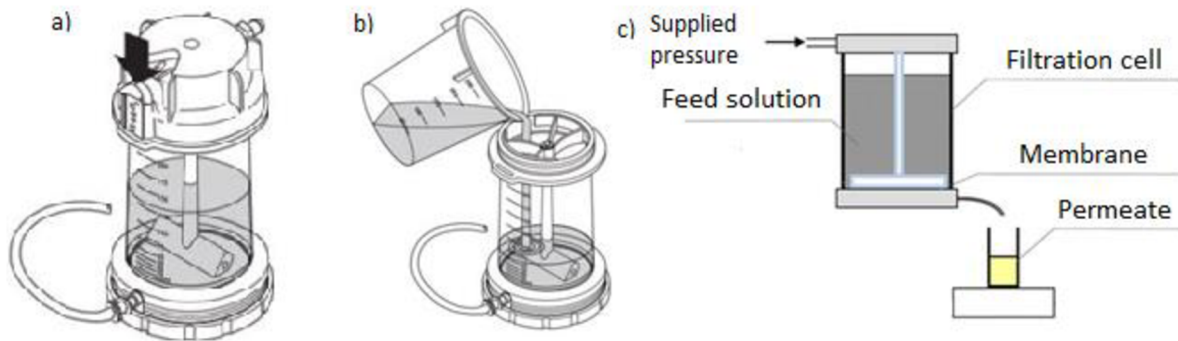


Figure 3-6 (a, b) Amicon Stirred Cell components and (c) dead end filtration cell schematic.

The compaction effect was caused by compressing asymmetric membrane under applied pressure, leads to decreasing the membrane transportation property [64]. Therefore, the investigated membranes became thinner and the filter flux were decreased gradually due to the compaction effect.

3.4.5.4 Calculation of flux, permeability and particle rejection rate

The permeating addresses for how much feed solution passing through the membrane. Therefore, the volumetric mass flow of fluid going through the membrane per unit area and per unit mass time is known as permeate flux. Moreover, following the Darcy's law, the permeate flux could linearly vary with membrane permeability and pressure which was supplied during the permeating process [65].

The permeate flux experiments were performed at room temperature and the permeation flux and the membrane permeability were calculated as below formulas [65,66]:

$$\text{Permeability} = \frac{\text{Permeate flux}}{\text{Applied pressure}}$$

$$J = \frac{\Delta V}{\Delta t * A}$$

- Permeability (unit in litre per square meter per hour per bar, L/h.m².bar) denoted for membrane permeability.
- J (unit in litre per square meter per hour, L/m².h) denoted for volumetric permeate flux.
- ΔV (unit in litre, L) denoted for permeate volume.
- Δt (unit in hour, h) denoted for permeate time.
- A (unit in square meter, m²) denoted for effective filtration area.

Turbidity rejection rate shows the quality of membrane filtration character since the higher rejection rate, the better filtration performance. It could be utilized to determine whether the

selected membrane could perform well in the particle separation process. The rejection rate was calculated as below formula:

$$\text{Particle rejection rate} = \frac{T_{\text{initial feed solution}} - T_{\text{permeate solution}}}{T_{\text{initial feed solution}}} \times 100\%$$

- Particle rejection rate (unit in percentage, %).
- $T_{\text{initial feed solution}}$ (unit in nephelometric turbidity units, NTUs) denoted for turbidity of initial feed solution of filtration test.
- $T_{\text{permeate solution}}$ (unit in nephelometric turbidity units, NTUs) denoted for turbidity of permeate solution of filtration test.

4 Results and Discussion

4.1 Membrane morphology by SEM images

Figures from 4-1 to 4-6 show the surface morphology and cross-section by SEM images for whole membrane samples from pristine PVDF, and blended PVDF with PVP or PEG additives.

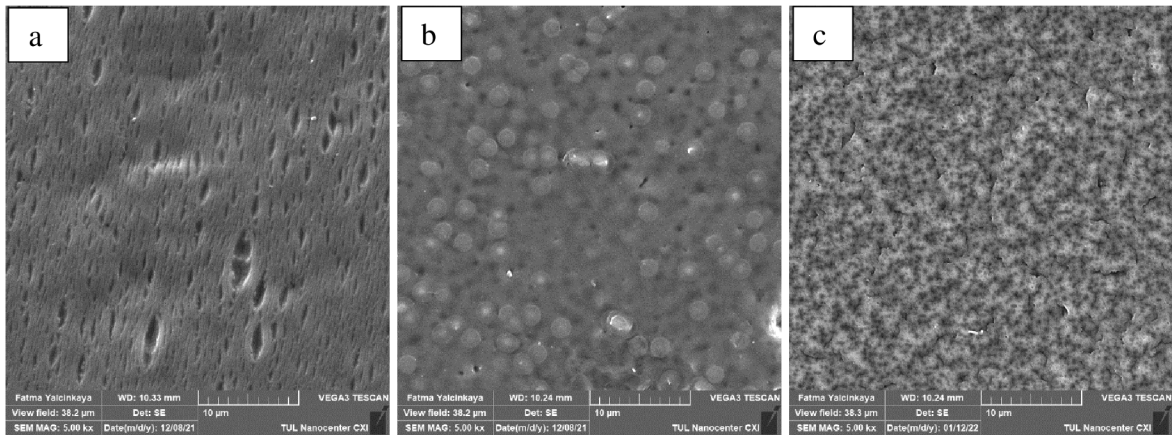


Figure 4-1 Surface morphology of pristine PDVF membranes by SEM images: a) PVDF10 b) PVDF15 c) PVDF20.

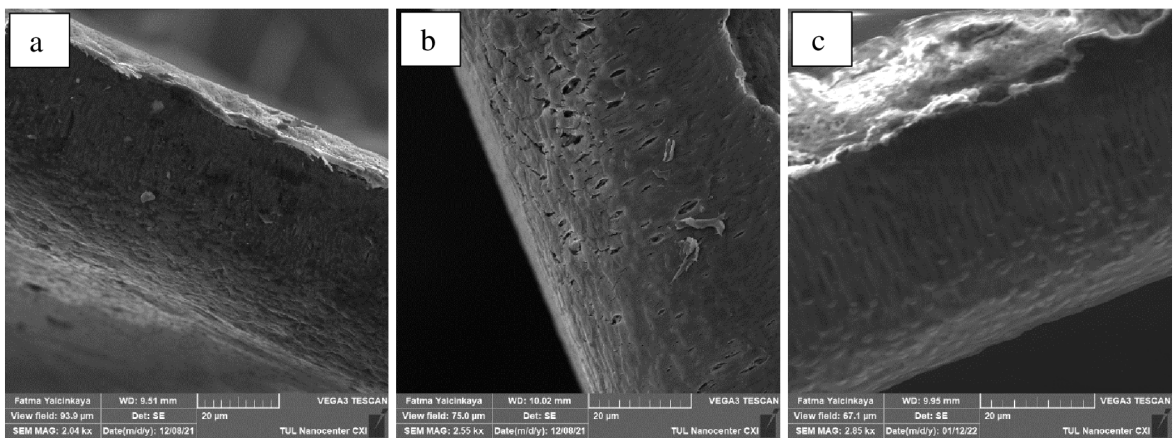


Figure 4-2 Cross-section of pristine PDVF membranes by SEM images: a) PVDF10 b) PVDF15 c) PVDF20.

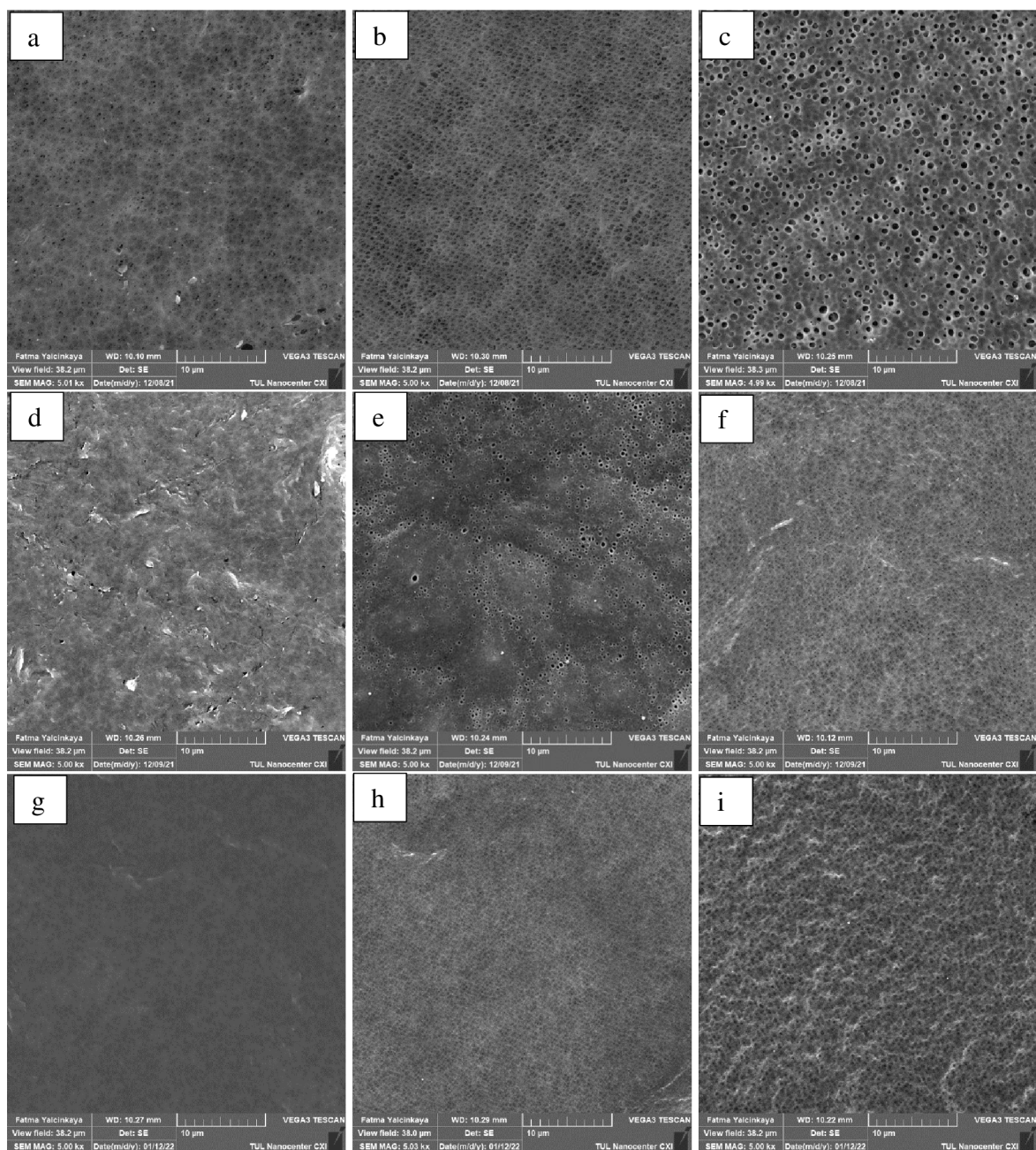


Figure 4-3 Surface morphology of blended PDVF with PVP additive membranes by SEM images: a) PVDF10/PVP2 b) PVDF10/PVP5 c) PVDF10/PVP8 d) PVDF15/PVP2 e) PVDF15/PVP5 f) PVDF15/PVP8 g) PVDF20/PVP2 h) PVDF20/PVP5 i) PVDF20/PVP8.

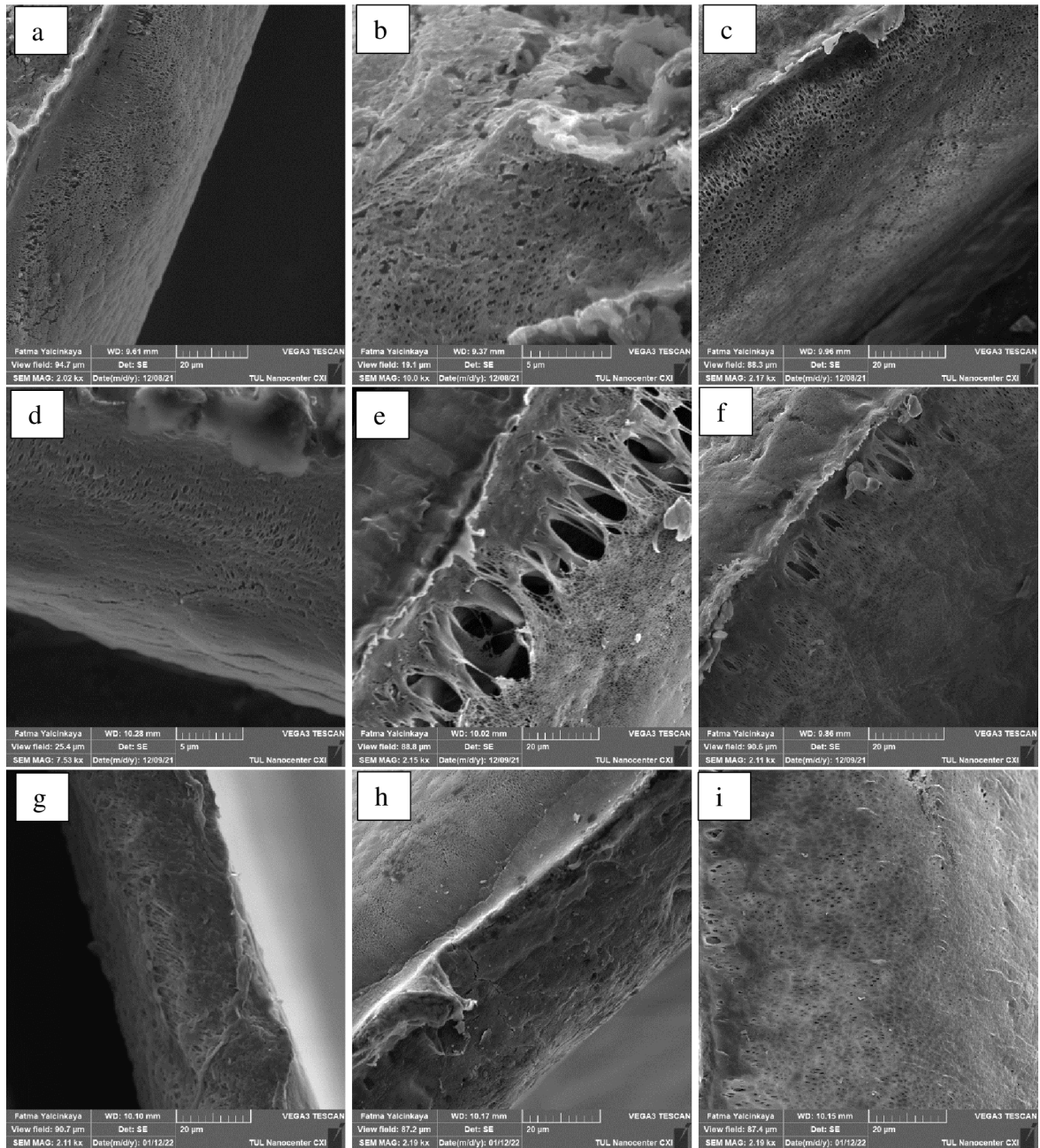


Figure 4-4 Cross-section of blended PDVF with PVP additive membranes by SEM images: a) PVDF10/PVP2 b) PVDF10/PVP5 c) PVDF10/PVP8 d) PVDF15/PVP2 e) PVDF15/PVP5 f) PVDF15/PVP8 g) PVDF20/PVP2 h) PVDF20/PVP5 i) PVDF20/PVP8.

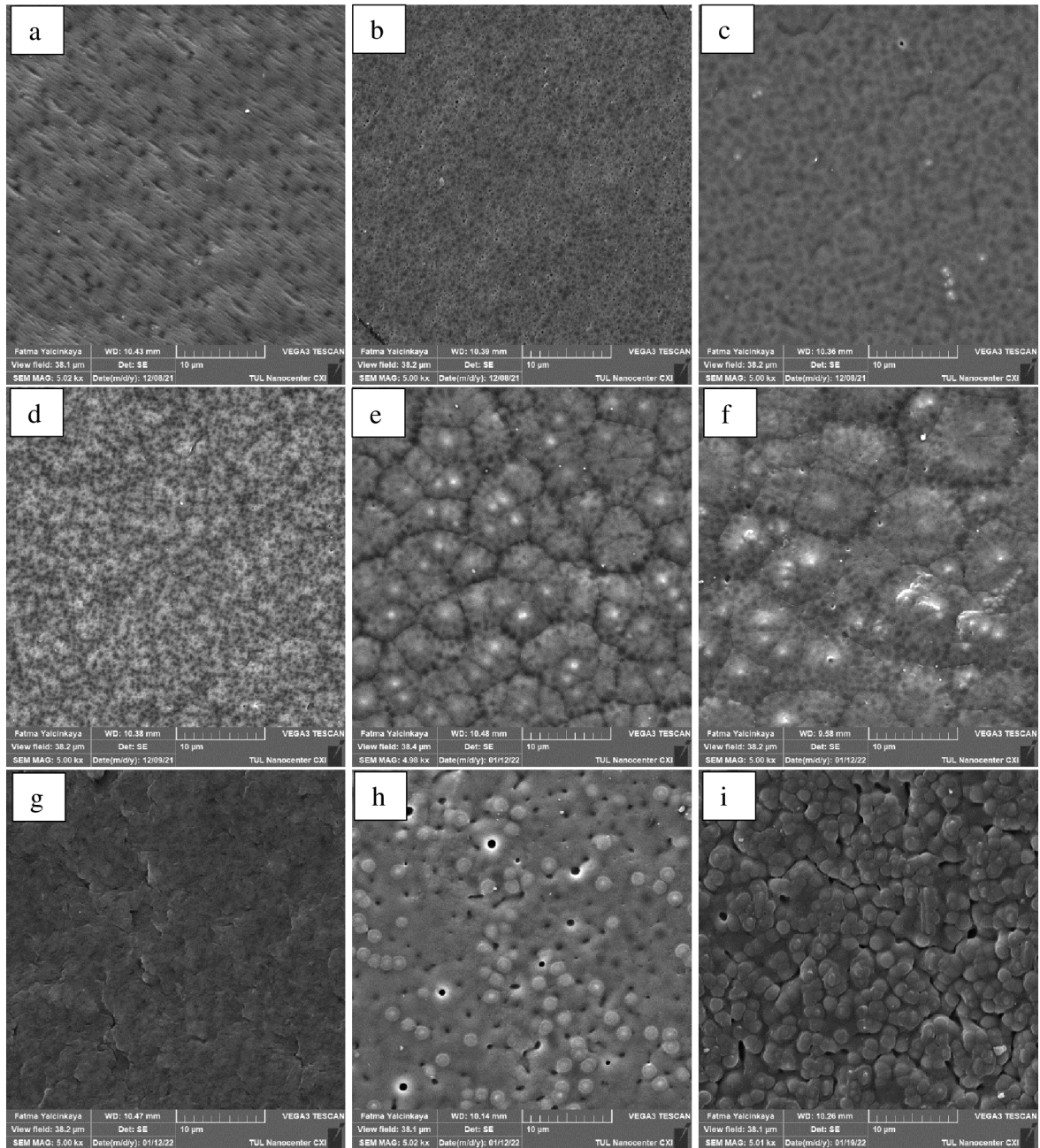


Figure 4-5 Surface morphology of blended PDVF with PEG additive membranes by SEM images: a) PVDF10/PEG2 b) PVDF10/PEG5 c) PVDF10/PEG8 d) PVDF15/PEG2 e) PVDF15/PEG5 f) PVDF15/PEG8 g) PVDF20/PEG2 h) PVDF20/PEG5 i) PVDF20/PEG8.

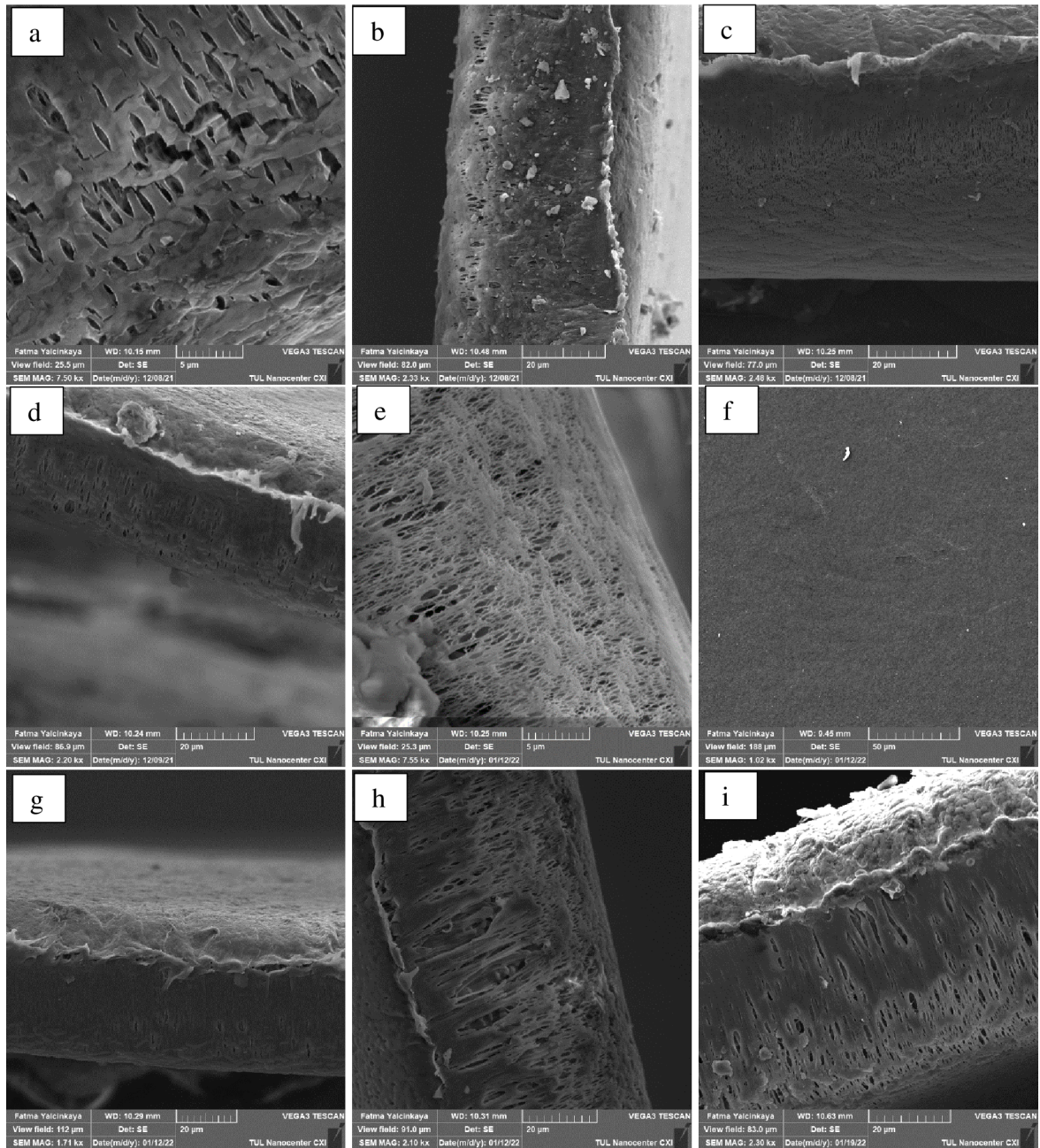


Figure 4-6 Cross-section of blended PDVF with PEG additive membranes by SEM images: a) PVDF10/PEG2 b) PVDF10/PEG5 c) PVDF10/PEG8 d) PVDF15/PEG2 e) PVDF15/PEG5 f) PVDF15/PEG8 g) PVDF20/PEG2 h) PVDF20/PEG5 i) PVDF20/PEG8.

Figures 4-1, 4-3 and 4-5 demonstrated the pristine PVDF membranes had smoother surface than the group of blended PDVF membranes.

With PVP and PEG acted as pore-forming agents, the blended membranes showed significant changing in the pores density and the pore dimension in figures 4-3 and 4-5, proved that the PVP

and PEG additives worked efficiently in membrane formation [2,14,44]. However, the additives might be partially leached away during NIPS process so the chemical analysis would be done by FTIR for each membranes.

The porous systems were observed in all prepared membrane in spite of they showed different morphology in figures 4-1, 4-3 and 4-5. Figures 4-1 and 4-3 showed the dense top layer with asymmetric surface morphology of pristine PVDF membrane and PVDF membrane blended with PVP, while the PVDF membrane blended with PEG showed sponge-like structures in figure 4-5.

Moreover, the roughness of prepared membranes was distinguishably different. It was believed that the surface roughness had positive correlation with bacterial deposition [67]. Therefore, decreasing membrane surface texture was supposed to increase anti fouling behavior and lead to better filtration performance of fabricated membranes. While the interchange of solvent and nonsolvent in NIPS process occurs in short time, the top layer of the casted film quickly precipitates right after immersion, it is not enough time for sublayer coarsening, bringing the polymer chains in dope solution do not sufficiently rearrange and result in surface roughness of prepared membranes [20].

Figures 4-2, 4-4 and 4-6 illustrated the macrovoid or sponge-like formation beneath the dense skin surface especially blended PVDF membranes. There were cavities in varied size and shape underneath the top layer and resulted in macrovoid channel in sublayer of fabricated membranes.

4.2 FTIR

Figures 4-7 to 4-13 show the results of the characterization using FTIR for whole membrane samples from only PVDF, PVDF with various compositions of PVP and PEG additives.

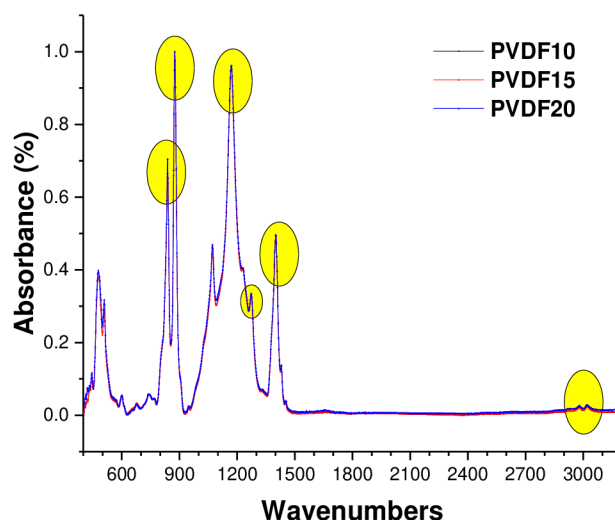


Figure 4-7 FTIR spectra of pristine PVDF membrane.

As is expected from FTIR results, there are no differences between the pristine PVDF10, PVDF15, and PVDF20 (Figure 4-7). The absorption bands at 3020 cm^{-1} and 2980 cm^{-1} corresponded to the $-\text{CH}_2$ asymmetric and symmetric vibration of PVDF [68]. The bands located at 1266 cm^{-1} and 1400 cm^{-1} were attributed to $-\text{CH}_2$ wagging vibration [68,69]. The absorption band at 840 cm^{-1} shows $-\text{CF}_2$ stretching [70]. The peak at 876 cm^{-1} corresponded to C–F groups of PVDF [68]. Stretching bands at 1170 cm^{-1} show the $-\text{CF}_2$ groups [68]. The band located at 1273 cm^{-1} is attributed to the vibration of C–F bonds [71].

In some papers, the absorption bands around 880 , 1071 , 1176 and 1400 cm^{-1} with high intensity were used to characterize the crystal phases of PVDF [72]. The symmetrical stretching bands of the $-\text{CF}_2$ group is indicated at 1071 cm^{-1} [59].

Figures 4-8, 4-9 and 4-10 are the FTIR spectra of PVDF – PVP blends. Besides the characteristic peaks of PVDF membrane, PVP was observed on the FTIR.

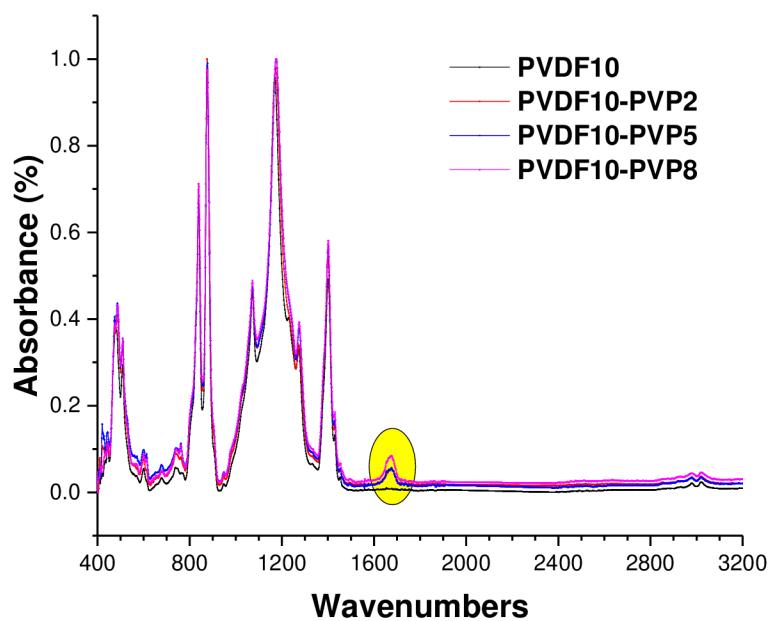


Figure 4-8 FTIR spectra of PVDF10/PVP membranes.

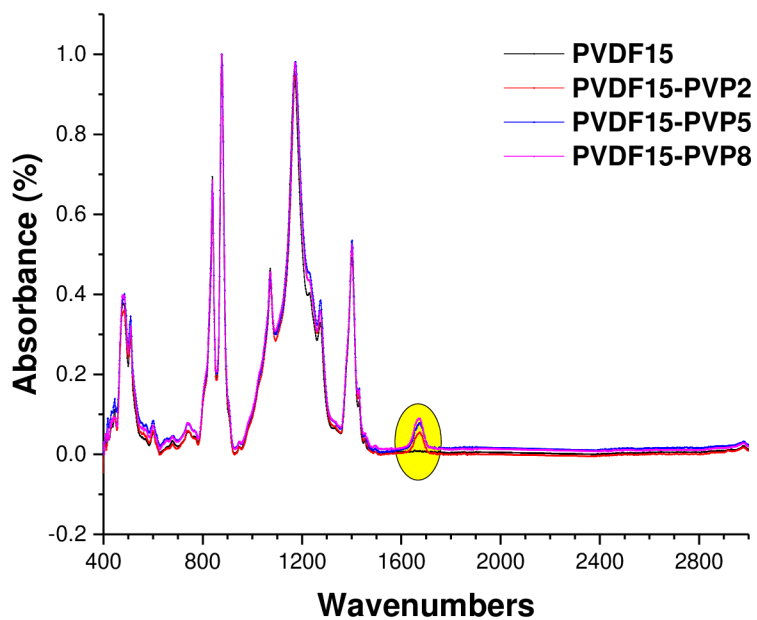


Figure 4-9 FTIR spectra of PVDF15/PVP membranes.

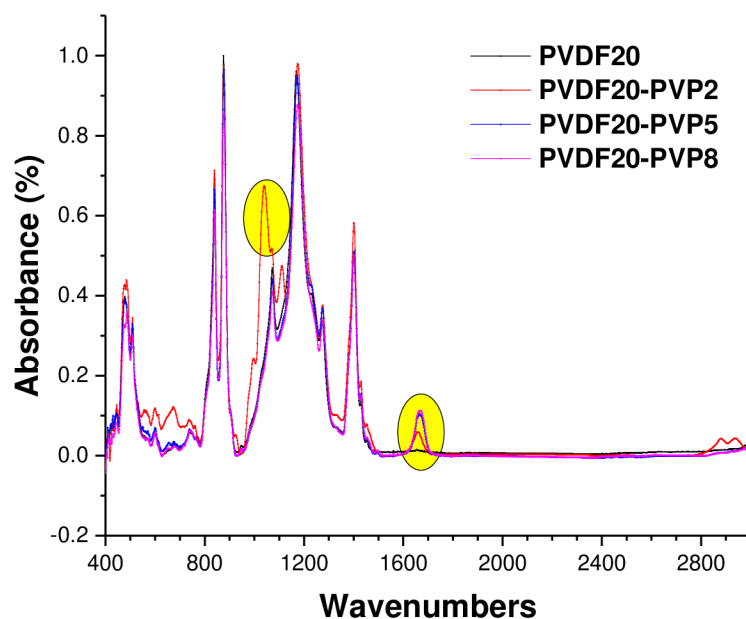


Figure 4-10 FTIR spectra of PVDF20/PVP membranes.

The carbonyl stretching absorption band of PVP at 1670 cm^{-1} shifts to higher frequencies of absorbance with the increase in the content of PVP. It was explained by the hydrogen bonding formation between the methylene group of PVDF and carbonyl group of PVP. The interaction of carbon and hydrogen of methylene in PVDF is weakened by hydrogen bonding. As a result, the absorption frequency of PVDF-methylene functional groups decreases and restricts in the vibration of C=O bands which allows to increases in PVB-carbonyl functional group's absorbance [70,73,74].

Surprisingly, PVDF20 – PVP2 shows strange shifter peaks at $1040, 1110, 2880,$ and 2940 cm^{-1} . It could be due to improper cleaning of membrane from glycerin and excessive solvent/salt remained on the membrane surface.

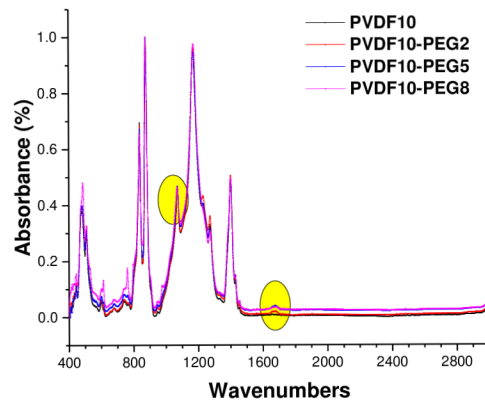


Figure 4-11 FTIR spectra of PVDF10/PEG membranes.

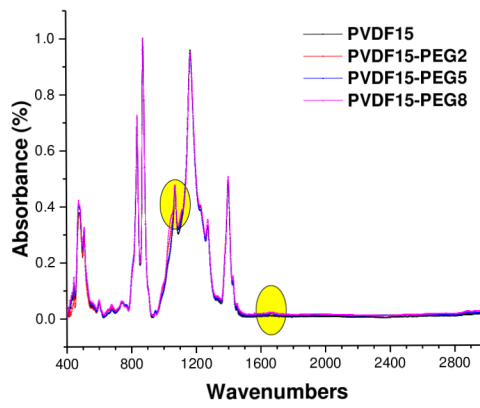


Figure 4-12 FTIR spectra of PVDF15/PEG membranes.

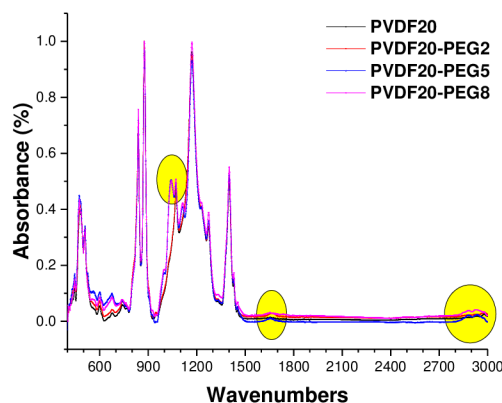


Figure 4-13 FTIR spectra of PVDF20/PEG membranes

FTIR images of PVDF – PEG membranes are shown in Figures 4-11, 4-12 and 4-13. As can be seen, the characteristics peaks of PVDF membranes appear at 1400, 1273, 1170, 840, and 876 cm^{-1} .

It was found that PEG hydrophilic additive can leach out from the cast film to the water nonsolvent during phase inversion [75]. 10 and 15 % wt. PVDF concentration did not show PEG characteristic peaks around 2915 and 2848 cm^{-1} . PEG (400Mn) has small molecular structure. It has probably smaller molecular structure than the solvent (DMAc, molar mass of 87.12 g/mol) [76]. The diffusion rate of the PEG molecule from the polymer-rich phase to the polymer lean phase is much higher than that of the DMAc solvent. As a result, PEG molecules can be easily washed out when immersion in water-nonsolvent due to the high diffusion rate during the phase inversion process.

At high concentration of PVDF (20% wt), the diffusion rate of the PEG molecule from the polymer-rich phase to the polymer lean phase is lower due to high viscosity and molecular chain entanglements of PVDF–PEG. As a result, the mobility of PEG molecules is restricted towards to the surface of the film and some PEG remained entrapped in the membrane matrix (Figure 4-13).

At highest concentration of PVDF (20% wt.), new peaks appeared around 2880 and 2920 cm^{-1} for 5 and 8% wt. of PEG. The peak around 2880 cm^{-1} indicates the stretching vibration of aliphatic $-\text{CH}_3$ functional group from PEG [77]. It was suggested that the intensity of peaks displayed around wavenumbers 2915 and 2848 cm^{-1} shows signify the presence of the PEG residual. These peaks correspond to stretching vibration of aliphatic CH_2 in the PEG [76]. The peak intensity is higher at higher PEG concentrations (5 and 8 % wt.), which means higher residual of PEG in the membrane matrix.

The FTIR spectrum of PVDF20 – PEG5 and PVDF20 – PEG8 blend shows some shifts in the band position (1071 cm^{-1} to 1040 cm^{-1}), band intensities and disappearance of other bands. These may be due to a good miscibility and specific interaction between fluorine in PVDF and carbon

connected to oxygen of PEG. In summary, the symmetrical stretching bands of the $-CF_2$ group is indicated at 1071 cm^{-1} shifted towards to 1040 cm^{-1} obviously after PEG grafting modification (Figure 4-13) [78]. The C–O stretching band (associated with PEG) at 1040 cm^{-1} is visible for the higher amount of PEG modification (5 and 8% wt.) and this proved that PEG remained in the membrane (Figure 4-13).

Overall results indicated that, mixture of PVDF/PVP is more visible under FTIR compared to PVDF/PEG. It could be due to easy leaching of PEG to nonsolvent during phase inversion process.

4.3 Membrane pore size and membrane thickness

Depending on the compositions of dope solutions (PVDF in DMAc or PVDF with PVP or PEG additives in DMAc) used to fabricate the membrane, significant variations pore size were observed. Table 4-1 shows the average pore dimension and average thickness for the prepared membranes (the Appendix A and Appendix B shows all measurements of pore size and membrane thickness, respectively).

Table 4-1 Average pore diameter data.

Sample No.	Sample abbreviation	Average pore size (in nanometer)	Average thickness (in micrometer)
1	PVDF - 10	356.620	27 ± 2.5
2	PVDF - 10 / PVP 2	99.127	38 ± 4
3	PVDF - 10 / PVP 5	68.958	81 ± 6.1
4	PVDF - 10 / PVP 8	152.138	11.4 ± 4.4
5	PVDF - 10 / PEG 2	181.923	49.8 ± 6.9
6	PVDF - 10 / PEG 5	110.055	38.4 ± 2.5
7	PVDF - 10 / PEG 8	367.002	64.3 ± 3.3
8	PVDF - 15	113.804	64.6 ± 2.1
9	PVDF - 15 / PVP 2	70.833	31.7 ± 2.6
10	PVDF - 15 / PVP 5	127.586	99.6 ± 12.2
11	PVDF - 15 / PVP 8	61.935	132.4 ± 17.3
12	PVDF - 15 / PEG 2	61.547	32.8 ± 1.3
13	PVDF - 15 / PEG 5	199.658	55.3 ± 1.8
14	PVDF - 15 / PEG 8	133.442	58 ± 2.3
15	PVDF - 20	308.525	46.8 ± 1.3
16	PVDF - 20 / PVP 2	104.098	27 ± 1
17	PVDF - 20 / PVP 5	95.243	102.3 ± 6.6
18	PVDF - 20 / PVP 8	94.496	169.9 ± 18.1
19	PVDF - 20 / PEG 2	103.231	43.7 ± 1.7
20	PVDF - 20 / PEG 5	391.267	78.6 ± 3.3
21	PVDF - 20 / PEG 8	275.761	70.6 ± 2.3

Overall, the membrane thickness got higher value along with the rise of additive content in polymeric solution, except the group PVDF10/PEG. However, table 4-1 showed that the membrane thickness fluctuated with the increase of PVDF concentration in pristine PVDF membranes. The membrane thickness firstly increased with the rise of PVDF content (PVDF10 at 27 μ m and PVDF15 at 64.6 μ m), and then decreased (PVDF15 at 64.6 μ m and PVDF20 at 46.8 μ m).

The membrane thickness varied inversely as its permeability, and an ideal membrane thickness in microfiltration is in the range 30 μ m to 60 μ m [65]. Therefore, it could be noted that most of fabricated membranes were suitable for microfiltration range in term of membrane thickness requirement.

All fabricated membranes were in the ultrafiltration to microfiltration range in term of pore dimension criterion.

Due to hydrophilic character of additive, the PVDF/PVP and PVDF/PEG blend membranes pore diameter normally opened and widened with increasing the additive concentration in dope solution.

However, the pore size of pristine PDVF membranes in three different contents were bigger than the others. This might be associated to the increasing of viscosity of casting solution. Higher viscosity of polymeric solution, hinders the interchanging of solvent and nonsolvent in NIPS, would postpone the process of macrovoids formation but increase the interconnect of pore matrix, simultaneously, the more complex of porous sublayer could lead to smaller pore size on top dense skin layer in membrane formation [79].

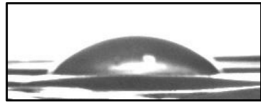
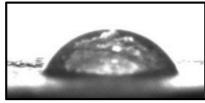
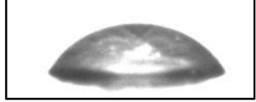
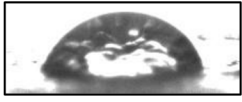
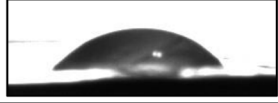
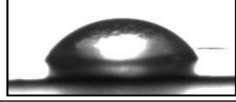

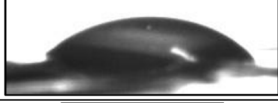
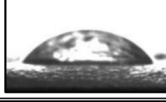
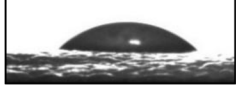
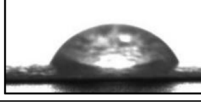
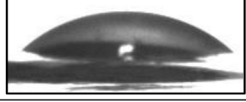
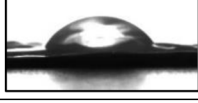
On the other hand, the PVDF/PVP and PVDF/PEG blend membranes resulted in a more dominating thermodynamic effect than a kinetic effect due to adding additive to polymeric solution, that led to higher porosity and narrower pore of fabricated membranes [80].

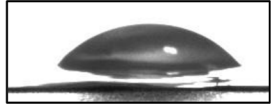

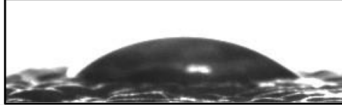
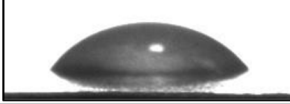
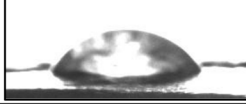

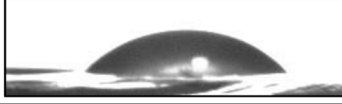
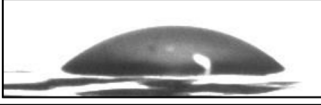
Because the membranes were dense, it was nearly impossible to identify the accurate pore size, therefore, the membrane still has to be examined with the permeability tests and rejection rate to determine the filtration property.

4.4 Contact angle

Table 4-2 shows the data of contact angle for all membrane samples using Drop Shape Analyzer for analyzing and capturing images.

Table 4-2 Contact angle data with images.

Sample No.	Sample abbreviation	Contact angle value (in degree)			Image
		Left side	Right side	Average	
1	PVDF - 10	44.3°	45.7°	45.0°	
2	PVDF - 10 / PVP 2	59.8°	59.8°	59.8°	
3	PVDF - 10 / PVP 5	59.7°	59.5°	59.6°	
4	PVDF - 10 / PVP 8	57.3°	56.1°	56.7°	
5	PVDF - 10 / PEG 2	52.0°	54.7°	53.4°	
6	PVDF - 10 / PEG 5	61.6°	61.5°	61.6°	
7	PVDF - 10 / PEG 8	60.0°	57.3°	58.7°	
8	PVDF - 15	45.6°	51.2°	48.4°	
9	PVDF - 15 / PVP 2	48.4°	48.4°	48.4°	
10	PVDF - 15 / PVP 5	74.4°	75.5°	75.0°	
11	PVDF - 15 / PVP 8	77.9°	77.4°	77.7°	
12	PVDF - 15 / PEG 2	46.7°	45.9°	46.3°	
13	PVDF - 15 / PEG 5	55.1°	56.1°	55.6°	

14	PVDF - 15 / PEG 8	52.2°	57.1°	54.7°	
15	PVDF - 20	49.2°	54.4°	51.8°	
16	PVDF - 20 / PVP 2	46.8°	45.1°	46.0°	
17	PVDF - 20 / PVP 5	57.5°	56.1°	56.8°	
18	PVDF - 20 / PVP 8	51.2°	52.6°	51.9°	
19	PVDF - 20 / PEG 2	40.7°	39.0°	39.9°	
20	PVDF - 20 / PEG 5	47.3°	49.9°	48.6°	
21	PVDF - 20 / PEG 8	41.6°	45.0°	43.3°	

The water contact angle value of pristine PVDF membrane was supposed to be higher than 85° [81], illustrated membrane hydrophobic character because of PVDF chemical property [25]. In this study measurements, the contact angle of pristine PVDF in 10%wt, 15%wt and 20%wt was 45°, 48.4° and 51.8°, respectively. The contact angle is a typical measurement to evaluate the hydrophilicity of the membrane surface [55,56]. However, the surface hydrophilicity was not only linked to contact angle, but also dependent on membrane surface morphology, surface smoothness, surface homogeneity and pore dimension [82]. It could be the main reason of the mobilized water contact angle value of pristine PVDF membranes as well as blended PVDF membranes in this study.

It was worth recalling that all fabricated membranes got the water contact angle under 90°, which tended to be hydrophilic nature of membrane surface [56]. The measurement values also registered a tendency that the water contact angle of the blended PVDF/PEG membranes were slightly lower than the blended PVDF/PVP membranes.

Because of the mobilizing in contact angle measurement, the membrane hydrophilicity could be examined with others test, such as water permeability tests or fouling test, etc.

4.5 Permeability and rejection rate

4.5.1 Water permeability performance for all membranes

Table 4-3 illustrates the data of water permeate flux and table 4-4 shows the calculation of water permeability performance for all membrane samples using Amicon dead-end filtration unit.

Table 4-3 Water permeate flux data.

Sample abbreviation	Permeate Volume (in liter)											
	0.011			0.021			0.031			0.0351		
	Time (in hour)	Pressure (in Bar)	Flux (in liter per hour per meter square)	Time (in hour)	Pressure (in Bar)	Flux (in liter per hour per meter square)	Time (in hour)	Pressure (in Bar)	Flux (in liter per hour per meter square)	Time (in hour)	Pressure (in Bar)	Flux (in liter per hour per meter square)
PVDF - 10	0.095	3.0	78.8	0.195	3.0	74.4	0.307	3.0	66.5	0.367	3.0	62.2
PVDF - 10 / PVP 2	0.001	0.500	6716.4	0.003	0.500	5373.1	0.004	0.500	3838.0	0.006	0.500	2686.6
PVDF - 10 / PVP 5	0.014	0.500	537.3	0.026	0.500	597.0	0.042	0.500	488.5	0.049	0.500	479.7
PVDF - 10 / PVP 8	0.009	0.500	790.2	0.021	0.500	655.3	0.034	0.500	584.0	0.041	0.500	537.3
PVDF - 10 / PEG 2	0.100	1.0	74.4	0.208	1.0	69.1	0.324	1.0	64.3	0.393	1.0	54.2
PVDF - 10 / PEG 5	0.015	1.0	506.9	0.032	1.0	426.4	0.046	1.0	526.8	0.054	1.0	479.7
PVDF - 10 / PEG 8	0.018	1.5	413.3	0.036	1.5	407.1	0.056	1.5	378.4	0.066	1.5	383.8
PVDF - 15	0.056	2.0	133.0	0.115	2.0	126.7	0.179	2.0	115.8	0.212	2.0	113.8
PVDF - 15 / PVP 2	0.014	0.5	537.3	0.033	0.5	389.4	0.055	0.5	344.4	0.066	0.5	335.8
PVDF - 15 / PVP 5	0.009	0.5	790.2	0.021	0.5	624.8	0.034	0.5	584.0	0.041	0.5	559.7
PVDF - 15 / PVP 8	0.011	0.5	688.9	0.023	0.5	639.7	0.036	0.5	571.6	0.042	0.5	559.7
PVDF - 15 / PEG 2	0.256	2.0	29.1	0.592	2.0	22.2	1.062	2.0	15.9	1.291	2.0	16.3

PVDF - 15 / PEG 5	0.269	1.0	27.8	0.800	1.0	14.1	1.336	1.0	13.9	1.612	1.0	13.5
PVDF - 15 / PEG 8	0.020	2.0	378.4	0.041	2.0	344.4	0.065	2.0	316.1	0.083	2.0	209.9
PVDF - 20	0.066	5.0	112.9	0.151	5.0	88.1	0.262	5.0	67.3	0.312	5.0	74.6
PVDF - 20 / PVP 2	0.009	0.5	790.2	0.021	0.5	671.6	0.041	0.5	363.0	0.056	0.5	244.2
PVDF - 20 / PVP 5	0.015	1.5	506.9	0.029	1.5	506.9	0.044	1.5	516.6	0.051	1.5	497.5
PVDF - 20 / PVP 8	0.013	1.0	597.0	0.026	1.0	548.3	0.040	1.0	537.3	0.047	1.0	516.6
PVDF - 20 / PEG 2	0.210	5.0	35.5	0.466	5.0	29.2	0.769	5.0	24.6	0.936	5.0	22.3
PVDF - 20 / PEG 5	0.113	5.0	65.8	0.234	5.0	61.9	0.371	5.0	54.6	0.442	5.0	52.1
PVDF - 20 / PEG 8	0	5.0	0.0	0	5.0	0.0	0	5.0	0.0	0	5.0	0.0

Table 4-4 Water permeability performance data.

Sample abbreviation	Permeability (in liter per square meter per hour per bar)			
	Permeate volume (in liter)			
	0.01l	0.02l	0.03l	0.035l
PVDF - 10	26.26	24.81	22.17	20.73
PVDF - 10 / PVP 2	13432.84	10746.27	7675.91	5373.13
PVDF - 10 / PVP 5	1074.63	1194.03	976.93	959.49
PVDF - 10 / PVP 8	1580.33	1310.52	1168.07	1074.63
PVDF - 10 / PEG 2	74.42	69.06	64.27	54.16
PVDF - 10 / PEG 5	506.90	426.44	526.78	479.74
PVDF - 10 / PEG 8	275.55	271.37	252.26	255.86
PVDF - 15	66.50	63.36	57.90	56.92
PVDF - 15 / PVP 2	1074.63	778.72	688.86	671.64
PVDF - 15 / PVP 5	1580.33	1249.57	1168.07	1119.40
PVDF - 15 / PVP 8	1377.73	1279.32	1143.22	1119.40
PVDF - 15 / PEG 2	14.57	11.11	7.93	8.16
PVDF - 15 / PEG 5	27.75	14.05	13.93	13.53
PVDF - 15 / PEG 8	189.19	172.22	158.03	104.94
PVDF - 20	22.58	17.62	13.47	14.93
PVDF - 20 / PVP 2	1580.33	1343.28	726.10	488.47
PVDF - 20 / PVP 5	337.93	337.93	344.43	331.67
PVDF - 20 / PVP 8	597.01	548.28	537.31	516.65
PVDF - 20 / PEG 2	7.10	5.83	4.93	4.46
PVDF - 20 / PEG 5	13.17	12.38	10.92	10.41
PVDF - 20 / PEG 8	0.00	0.00	0.00	0.00

The water permeability performance for all fabricated membranes in table 4-4 was calculated from permeate flux data as equation mentioned in part 3.4.5.4.

For better observation, figures 4-14, 4-15 and 4-16 visualized the water permeability for three different groups of prepared membranes: pristine PVDF10 and blended PVDF10 membranes, pristine PVDF15 and blended PVDF15 membranes and pristine PVDF20 and blended PVDF20 membranes.

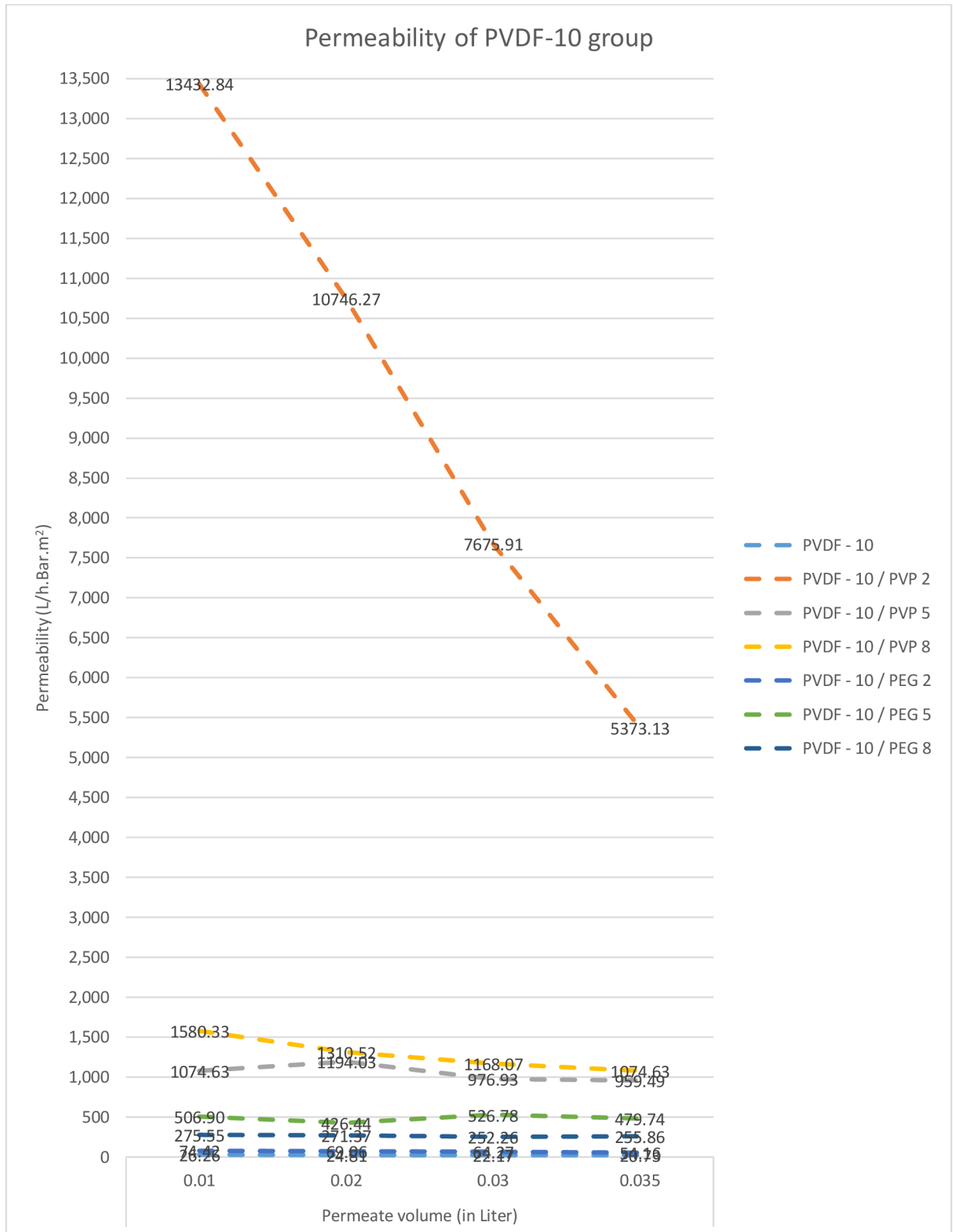


Figure 4-14 Water permeability of PVDF10 group.

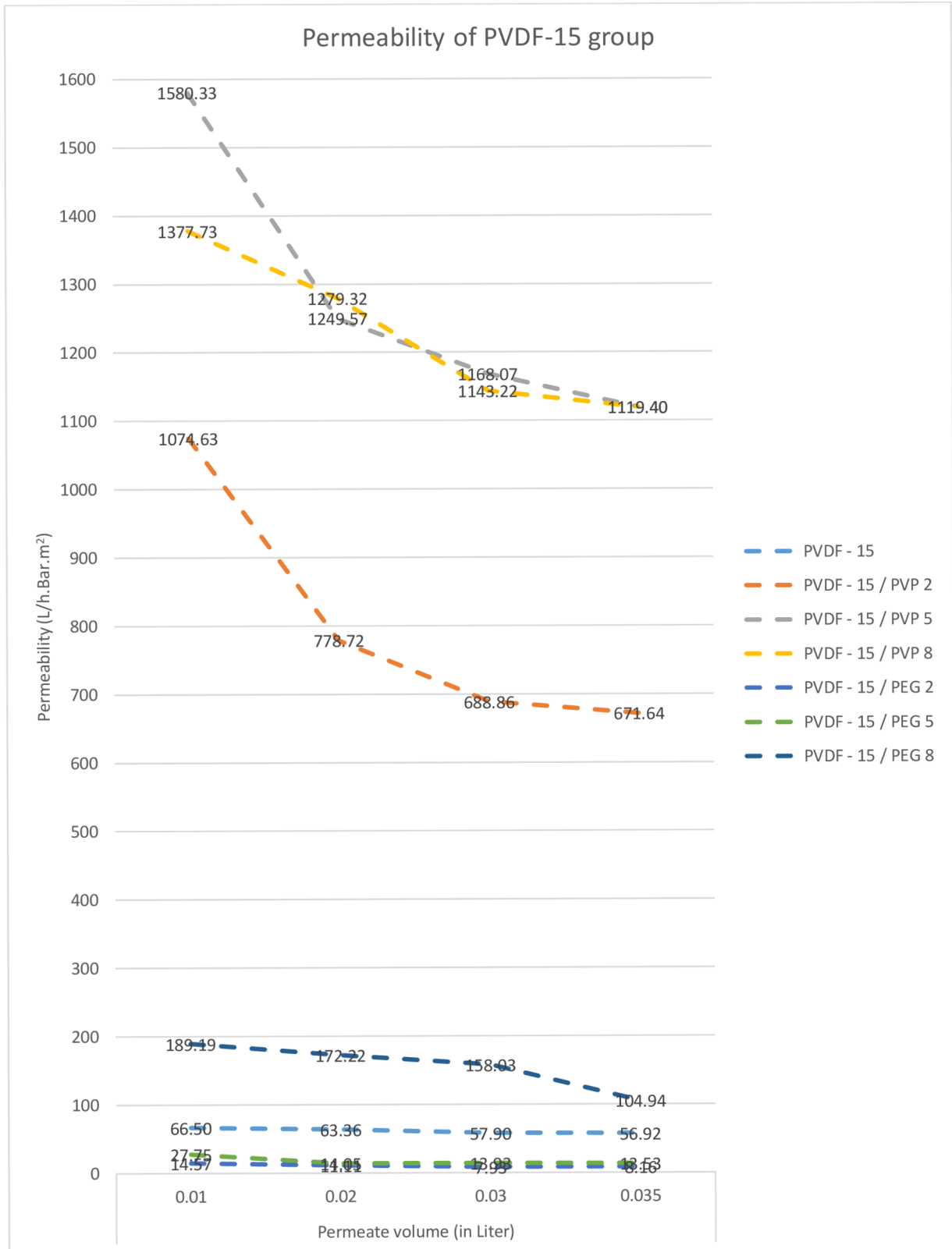


Figure 4-15 Water permeability of PVDF15 group.

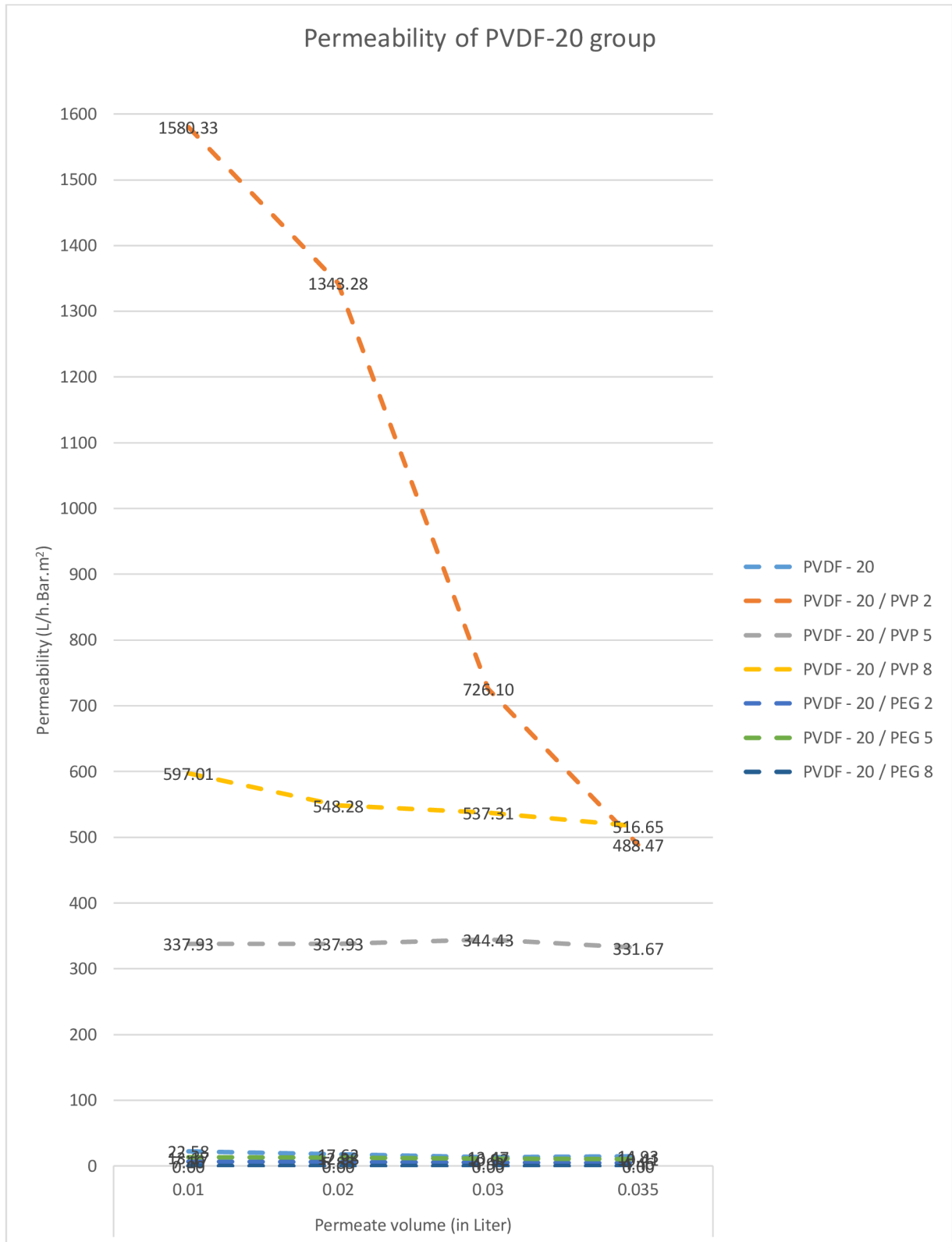


Figure 4-16 Water permeability of PVDF20 group.

The good transport media directly reflected the higher hydrophilicity of membranes. In many studies, increasing the hydrophilic groups in a membrane by adding PVP or PEG additives could proportionally increase its hydrophilicity and result in better permeability performance [5,8, 47,48]. While average pore dimension, membrane thickness and membrane porosity, and contact angle also positively contributed to membrane permeability performance.

Overall, most of membranes registered the expect result, the water permeability performance got higher value along with the rise of additive content in polymeric solution, showed in table 4-4. However, while the PVP group saw a reliable increase in the permeability, the opposite trend was found when PEG was added.

There were two effects happening simultaneously and against each other in membrane formation. Additives acted as pore-forming agent, so if their concentrations witnessed a rise, following the rise in permeability [5,8, 47,48]. Increasing the PVDF content or adding PVP and PEG additives apparently increased the viscosity of polymeric solution, higher viscosity hindered macrovoids formation and led to smaller pore size on top dense skin layer in membrane formation and decreased the permeability [79]. So that adding hydrophilicity agents like PVP and PEG would increase the membrane permeability until a certain content was reached. Many researches demonstrated the turning point in permeability might vary depending on the type of polymer and its concentration as well as the used additive.

Table 4-4 also showed that the water permeability value fluctuated with the increase of PVDF concentration in pristine PVDF membranes as well as the increase of additive content in blended PVDF membranes. For example, the water permeability firstly increased with the rise of PVDF content (PVDF10 at $20.73 \text{ mL}/\text{m}^2 \cdot \text{h} \cdot \text{Bar}$ and PVDF15 at $56.92 \text{ mL}/\text{m}^2 \cdot \text{h} \cdot \text{Bar}$), and then decreased (PVDF15 at $56.92 \text{ mL}/\text{m}^2 \cdot \text{h} \cdot \text{Bar}$ and PVDF20 at $14.93 \text{ mL}/\text{m}^2 \cdot \text{h} \cdot \text{Bar}$). The water contact angle of PVDF 20 is comparable higher than others which might decrease the water permeability. On the other hand, the water contact angle of PVDF10 and PVDF15 is almost the same. In this case, pore size and porosity can play predominant effect on water permeability

It was important to note that PVDF10/PVP group witnessed a sharp increase in the water permeability and made it the most efficient membrane among the others membrane group. It is proved that PVDF10/PVP group outperformed with the rest and the highest value was obtained for PVDF10/PVP2 membrane. PVP is used to increase porosity, mechanical properties, and α -to- β phase transformation of membrane. PVP can induce the building of pore structure which can affect the porosity of overall membrane. Even though the PVP leaches out partly from non-solvent, some of them remains trapped in the membrane network and keep membrane inner hydrophilicity [83].

In contrast, PVDF15/PEG group and PVDF20/PEG group showed the lower number in permeability, accounting for only one-quarter or lower of the pristine PVDF15 and PVDF20, respectively. Moreover, PVDF20/PEG8 was water impermeable at 5.0 Bar.

Moreover, membranes under high pressure filtration process were affected by the compaction effect due to membrane fouling and membrane structure collapsing. The compaction effect caused difficulty for the flux transports through membrane pore system, resulted in the loss of membrane permeability, explained why the permeability decreased when permeate volume increased for each type of membrane [84].

4.5.2 Permeability performance and rejection rate of selected membranes by different pollutant solutions

The pristine PVDF could be a stable membrane against a wide range of harsh chemicals [2,29,36], and the PVDF10/PVP group demonstrated a promising result in micro filtration, therefore, they were chosen for further process.

The selected membranes were under the filtration experiments using Amicon dead-end filtration unit with prepared pollutant solutions.

Table 4-5, 5-6 and 4-7 illustrate the data of three different pollutant solutions permeate flux and table 4-8 shows the calculation of permeability performance for selected membranes.

Table 4-5 Permeability performance of selected membranes by water-soluble pollutants with 0.1 μ m diameter.

Sample abbreviation	Permeate Volume (in liter)											
	0.011			0.021			0.031			0.0351		
	Time (in hour)	Pressure (in Bar)	Flux (in liter per hour per meter square)	Time (in hour)	Pressure (in Bar)	Flux (in liter per hour per meter square)	Time (in hour)	Pressure (in Bar)	Flux (in liter per hour per meter square)	Time (in hour)	Pressure (in Bar)	Flux (in liter per hour per meter square)
PVDF - 10	0.007	2.0	1074.6	0.015	2.0	895.5	0.026	2.0	671.6	0.032	2.0	671.6
PVDF - 10 / PVP 2	0.003	0.25	2985.1	0.006	0.25	2238.8	0.010	0.25	1919.0	0.012	0.25	1919.0
PVDF - 10 / PVP 5	0.002	0.25	4477.6	0.004	0.25	3838.0	0.006	0.25	3358.2	0.009	0.25	1033.3
PVDF - 10 / PVP 8	0.003	0.25	2442.3	0.006	0.25	2442.3	0.009	0.25	2686.6	0.010	0.25	3358.2
PVDF - 15	0.011	2.0	688.9	0.022	2.0	655.3	0.042	2.0	383.8	0.061	2.0	191.9
PVDF - 20	-	4.0	0.0	-	4.0	0.0	-	4.0	0.0	-	4.0	0.0

Table 4-6 Permeability performance of selected membranes by water-soluble pollutants with 0.2 μ m diameter.

Sample abbreviation	Permeate Volume (in liter)											
	0.011			0.021			0.031			0.0351		
	Time (in hour)	Pressure (in Bar)	Flux (in liter per hour per meter square)	Time (in hour)	Pressure (in Bar)	Flux (in liter per hour per meter square)	Time (in hour)	Pressure (in Bar)	Flux (in liter per hour per meter square)	Time (in hour)	Pressure (in Bar)	Flux (in liter per hour per meter square)
PVDF - 10	0.029	3.5	255.9	0.064	3.5	214.9	0.099	3.5	209.9	0.118	3.5	197.5
PVDF - 10 / PVP 2	0.003	0.25	2238.8	0.008	0.25	1791.0	0.011	0.25	1919.0	0.014	0.25	1343.3

PVDF - 10 / PVP 5	0.004	0.25	1919.0	0.008	0.25	1919.0	0.012	0.25	1679.1	0.015	0.25	1492.5
PVDF - 10 / PVP 8	0.002	0.25	3358.2	0.005	0.25	2985.1	0.008	0.25	2686.6	0.010	0.25	1679.1
PVDF - 15	0.067	3.5	111.0	0.129	3.5	121.0	0.196	3.5	111.0	0.222	3.5	142.9
PVDF - 20	-	4.0	0.0	-	4.0	0.0	-	4.0	0.0	-	4.0	0.0

Table 4-7 Permeability performance of selected membranes by water-soluble pollutants with 0.5 μ m diameter.

Sample abbreviation	Permeate Volume (in liter)											
	0.011			0.021			0.031			0.0351		
	Time (in hour)	Pressure (in Bar)	Flux (in liter per hour per meter square)	Time (in hour)	Pressure (in Bar)	Flux (in liter per hour per meter square)	Time (in hour)	Pressure (in Bar)	Flux (in liter per hour per meter square)	Time (in hour)	Pressure (in Bar)	Flux (in liter per hour per meter square)
PVDF - 10	0.078	3.5	95.9	0.167	3.5	83.4	0.284	3.5	64.0	0.342	3.5	64.0
PVDF - 10 / PVP 2	0.002	0.5	3838.0	0.004	0.5	3358.2	0.006	0.5	3358.2	0.008	0.5	3358.2
PVDF - 10 / PVP 5	0.002	0.5	3358.2	0.005	0.5	2985.1	0.007	0.5	2985.1	0.009	0.5	2238.8
PVDF - 10 / PVP 8	0.002	0.5	3358.2	0.005	0.5	2686.6	0.009	0.5	2066.6	0.011	0.5	1919.0
PVDF - 15	0.069	2.0	108.3	0.156	2.0	85.3	0.273	2.0	64.1	0.323	2.0	74.6
PVDF - 20	0.039	3.5	191.9	0.083	3.5	169.0	0.145	3.5	121.0	0.184	3.5	95.3

Table 4-8 Permeability performance and rejection rate of selected membranes by water-soluble pollutants solution.

Filtration solution	Permeability (in liter per square meter per hour per bar)				Turbidity of filtered solution	Rejection rate	
	Sample abbreviation	Permeate volume (in liter)					
		0.01l	0.02l	0.03l			0.035l
Water-soluble pollutants with 0.1µm diameter	PVDF - 10	537.31	447.76	335.82	335.82	5.60	48.6%
	PVDF - 10 / PVP 2	11940.30	8955.22	7675.91	7675.91	3.02	72.3%
	PVDF - 10 / PVP 5	17910.45	15351.81	13432.84	4133.18	2.23	79.5%
	PVDF - 10 / PVP 8	9769.34	9769.34	10746.27	13432.84	9.22	15.4%
	PVDF - 15	344.43	327.63	191.90	95.95	8.22	24.6%
	PVDF - 20	0.00	0.00	0.00	0.00	10.90	0.0%
Water-soluble pollutants with 0.2µm diameter	PVDF - 10	73.10	61.41	59.97	56.44	43.80	49.6%
	PVDF - 10 / PVP 2	8955.22	7164.18	7675.91	5373.13	52.90	39.1%
	PVDF - 10 / PVP 5	7675.91	7675.91	6716.42	5970.15	63.20	27.3%
	PVDF - 10 / PVP 8	13432.84	11940.30	10746.27	6716.42	8.81	89.9%
	PVDF - 15	31.72	34.58	31.72	40.83	44.70	48.6%
	PVDF - 20	0.00	0.00	0.00	0.00	86.90	0.0%
Water-soluble pollutants with 0.5µm diameter	PVDF - 10	27.41	23.84	18.28	18.28	40.60	31.1%
	PVDF - 10 / PVP 2	7675.91	6716.42	6716.42	6716.42	48.00	18.5%
	PVDF - 10 / PVP 5	6716.42	5970.15	5970.15	4477.61	37.90	35.7%
	PVDF - 10 / PVP 8	6716.42	5373.13	4133.18	3837.95	43.30	26.5%
	PVDF - 15	54.16	42.64	32.06	37.31	47.20	19.9%
	PVDF - 20	54.83	48.28	34.58	27.22	51.80	12.1%

Generally, the permeability performance by pollutant solutions maintained the similar trend with water permeability. The PVDF10/PVP group continuously performed well but PVDF20 membrane was impermeable at 4.0 Bar with solution of 0.1 μ m and 0.2 μ m diameter pollutants.

Turbidity rejection rate shows the quality of membrane filtration character since the higher rejection rate, the better filtration performance. The rejection rate of selected membranes fluctuated when increased the PVDF as well as PVP content. The rejection rate also could not register any correlation with the permeability value. In size exclusion filtration, the rejection rate experiences a similar trend with the permeability value [85]. It is because both permeability and rejection rate mainly depends on the membrane pore size and its pore size distribution as well as membrane porosity, especially the data of top layer [85]. However, the relation could vary inversely due to the absorptive effect and membrane sublayer structure [4].

The best rejection rate was PVDF10/PVP8 at 89.9% with 0.2 μ m diameter pollutants, much better than 0.1 μ m and 0.5 μ m diameter pollutants solution at 15.4% and 26.5%, respectively. The filtered quality of selected membranes with 0.5 μ m diameter pollutants were not good enough, all rejection rates were registered below 35%.

4.6 Water uptake and swelling degree

Table 4-9 shows the data of water uptake and table 4-10 demonstrates the data of swelling degree for six selected membranes.

Table 4-9 Water uptake data.

Sample abbreviation	Average weight in dry form (in gram)	Average weight in wet form (in gram)	Water uptake (in percentage)
PVDF - 10	0.0168	0.0251	49.4%
PVDF - 10 / PVP 2	0.0166	0.0350	110.8%
PVDF - 10 / PVP 5	0.0134	0.0628	368.7%
PVDF - 10 / PVP 8	0.0183	0.0928	407.1%
PVDF - 15	0.0273	0.0323	18.0%
PVDF - 20	0.0447	0.0493	10.2%

Table 4-10 Swelling degree data

Sample abbreviation	Area in dry form (in cm^2)	Average area in wet form (in cm^2)	Swelling degree (in percentage)
PVDF - 10	9.0	8.2133	8.7%
PVDF - 10 / PVP 2	9.0	8.4000	-6.7%
PVDF - 10 / PVP 5	9.0	8.1200	-9.8%
PVDF - 10 / PVP 8	9.0	9.3000	3.3%
PVDF - 15	9.0	8.5067	-5.5%
PVDF - 20	9.0	8.9900	-0.1%

Membrane water uptake measurement demonstrates the water adsorption ability of membrane which is a crucial characteristic in filtration technology [58,59]. Moreover, a high water uptake according to more inner space of sublayer, leads to better water transportation as well as filtration performance [60].

As expected, the PVDF10/PVP group continuously outperformed compared with pristine PVDF membrane, this result proved that PVP additive was known for high water uptake. The PVDF10/PVP8 registered the highest value, at 407.1%, showed a good transport for both water and pollutant solutions (due to high permeability value for both water and pollutant solutions showed in table 4-4 and 4-8).

The water uptake also varied inversely with the increasing of PVDF concentration, PVDF10, PVDF 15 and PVDF20 had water uptake at 49.4%, 18% and 10.2%, respectively. It could be explained due to the increasing of polymeric viscosity. The increasing of viscosity in polymeric solution hindered macrovoids formation and decreased the permeability [79], led to the decreasing of water uptake value.

Meanwhile, the swelling degree of PVDF10/PVP group was greater than pristine PVDF. However, PVDF10/PVP8 was the second lowest compared with others selected membranes, at 3.3%. The diminished swelling ratio increases the rigidity of voids formation in membrane matrix [60], that means better membrane stability for PVDF10/PVP8.

5 Conclusion and Recommendations

In this study, three pristine PVDF, eighteen blended PVDF membranes in varied concentrations were prepared by NIPS method using DMAc solvent while PVP and PEG were used as hydrophilic additives. The type of additive, the PVDF content, the blending ratio between PVDF and additive were directly effect to fabricated membranes [18].

The membranes were fabricated and characterized. The investigations included the morphology and pore size by SEM image, chemical property by FTIR, their hydrophilicity and filtration performance by contact angle, transport flux, permeability, water uptake and rejection rate, as well as their stability by swelling ratio.

In this study, SEM images showed that fabricated membranes had the dense skin on top layer and macrovoid in sublayer due to NIPS method, created fairly good channel for transport media. The interchanging between solvent and non-solvent resulted in asymmetric membrane structures [20]. Because of asymmetric structure, ones part in top skin worked as actively filtering layer while others parts in cross-section worked as a mechanical supporter [10].

As expected, pristine PVDF membranes tended to low rejection ability, hydrophobic character with low permeability, and less functional group (only $-CH_2$ group was found by FTIR result). PVP additive improved the hydrophilicity of blended PVDF/PVP membranes, which was reflected in the permeability performance as well as water uptake value. Besides that, blended PVDF membrane with PEG additive could not bring the promising result. It could be explained as PEG was leached out from the blended membrane during phase inversion process [75] (based on FTIR result).

The main conclusions are:

- NIPS method could form the asymmetric membrane with random pore distribution, enhanced its transport media, made it more suitable to separate microplastics in microfiltration.
- Increasing the content of dope solution in NIPS process could affect to the membrane formation, the positive result only came when the suitable concentration and condition were found. This statement was applied for both main polymer and additive in dope solution.
- The turning point in membrane properties might vary depending on the type of main polymer and its concentration as well as the used additive for the system.
- Adding PEG additive could not bring in clear effect on membrane property, it could because PEG in blended PVDF/PEG membranes was leached out mostly in this study.
- Adding PVP to dope solution attributed to the promising results with significantly improving in permeability. It was worth recalling that increasing PVP content could not result in the proportional increasing membrane properties.
- Group PVDF10/PVP outperformed in permeability.

- When membrane was used to filter, the compaction effect occurred subsequently. It induced the instability of membrane structure and led to pore system collapsing as well as decrease permeability performance.

The obtained results suggested that there were six out of twenty-one membranes were good enough for further step, including pristine PVDF membranes and blended PVDF10/PVP membranes group. The permeability and rejection rate of selected membranes were investigated simultaneously. As expected, the result of PVP10/PVP was much better than pristine PVDF group and the PVP10/PVP8 performed the best among selected membranes.

Unfortunately, the selected membranes seemed to have a negative result in rejection rate. It was presumed that the membranes with randomly large pores distribution or cracking/damage could fail in rejection test.

Moreover, it was worth finding that the membrane mechanical properties decreased in time while keeping in both water and Glycerin [16]. Most of the membranes were easily torn up after times, therefore all the experiments were conducted with freshly fabricated membrane to maintain the quality and consistence for final test results.

This study still demonstrated the potential advantage of adding PVP additive in PVDF membrane formation by NIPS method. For this reason, the selected membrane performance could still be improved by surface modification, it might conduct a better membrane with higher rejection rate and better mechanical property.

- Bibliography

- [1] Membranes Market Global Forecast to 2024 | MarketsandMarkets, MarketsandMarkets™, 2020. <https://www.marketsandmarkets.com/Market-Reports/membranes-market-1176.html> (accessed March 19, 2022).
- [2] C. Sun, X. Feng, Enhancing the performance of PVDF membranes by hydrophilic surface modification via amine treatment, *Separation and Purification Technology*. 185 (2017) 94–102. <https://doi.org/10.1016/j.seppur.2017.05.022>.
- [3] L. Broens, F. Altena, C. Smolders, D. Koenhen, Asymmetric membrane structures as a result of phase separation phenomena, *Desalination*. 32 (1980) 33–45.
- [4] C. Kahrs, J. Schwellenbach, Membrane formation via non-solvent induced phase separation using sustainable solvents: A comparative study, *Polymer*. 186 (2020) 122071. <https://doi.org/10.1016/j.polymer.2019.122071>.
- [5] F. Santoso, Untersuchungen zur simultanen Aminierung und Porenöffnung von Polyetherimid-Membranen, (2004).
- [6] H. Lonsdale, The growth of membrane technology, *Journal of Membrane Science*. 10 (1982) 81–181.
- [7] X. Li, B.R. Jasti, eds., *Design of controlled release drug delivery systems*, McGraw-Hill, New York, 2006.
- [8] H. Strathmann, Membrane separation processes, *Journal of Membrane Science*. 9 (1981) 121–189.
- [9] A review of polymeric membranes and processes for potable water reuse | Elsevier Enhanced Reader, (n.d.). <https://doi.org/10.1016/j.progpolymsci.2018.01.004>.
- [10] S. Loeb, S. Sourirajan, *Sea water demineralization by means of an osmotic membrane*, in: ACS Publications, 1962.
- [11] M.K. Purkait, M.K. Sinha, P. Mondal, R. Singh, Chapter 1 - Introduction to Membranes, in: M.K. Purkait, M.K. Sinha, P. Mondal, R. Singh (Eds.), *Interface Science and Technology*, Elsevier, 2018: pp. 1–37. <https://doi.org/10.1016/B978-0-12-813961-5.00001-2>.
- [12] X. Dong, A.R.A. Al-Jumaily, I.C. Escobar, Investigation of the Use of a Bio-Derived Solvent for Non-Solvent-Induced Phase Separation (NIPS) Fabrication of Polysulfone Membranes, *Membranes*. 8 (2018).
- [13] A. Shelekhin, E. Grosogeat, S. Hwang, Preparation and Characterization of Inorganic Membranes, in: *Trans Tech Publ*, 1992: pp. 1–10.
- [14] R. Lusiana, V. Sangkota, N. Sasongko, G. Gunawan, A. Wijaya, S. Santosa, D. Siswanta, M. Mudasir, M.N. Zainol Abidin, S. Mansur, M.H. Othman, Permeability improvement of polyethersulfone-polyethylene glycol (PEG-PES) flat sheet type membranes by tripolyphosphate-

crosslinked chitosan (TPP-CS) coating, *International Journal of Biological Macromolecules*. 152 (2020). <https://doi.org/10.1016/j.ijbiomac.2020.02.290>.

[15] R. Bertera, H. Steven, M. Metcalfe, Development studies of crossflow microfiltration, *Chemical Engineer (London)*. (1984) 10–14.

[16] J.U.M. Garcia, *Understanding Membrane Formation in Nonsolvent-Induced Phase Separation*, University of California, Santa Barbara, 2020.

[17] R. Kesting, A. Fritzsche, M. Murphy, C. Cruse, A. Handermann, R. Malon, M. Moore, The second-generation polysulfone gas-separation membrane. I. The use of lewis acid: base complexes as transient templates to increase free volume, *Journal of Applied Polymer Science*. 40 (1990) 1557–1574.

[18] M.K. Purkait, R. Singh, *Membrane technology in separation science*, CRC Press, 2018.

[19] M.K. Purkait, M.K. Sinha, P. Mondal, R. Singh, *Stimuli responsive polymeric membranes: smart polymeric membranes*, Academic Press, 2018.

[20] J.G. Wijmans, C.A. Smolders, Preparation of Asymmetric Membranes by the Phase Inversion Process, in: P.M. Bungay, H.K. Lonsdale, M.N. de Pinho (Eds.), *Synthetic Membranes: Science, Engineering and Applications*, Springer Netherlands, Dordrecht, 1986: pp. 39–56. https://doi.org/10.1007/978-94-009-4712-2_2.

[21] N. Nady, N. Salem, S.H. Kandil, Preparation and Characterization of a Novel Poly(vinylidene fluoride-co-hexafluoropropylene)/Poly(ethersulfone) Blend Membrane Fabricated Using an Innovative Method of Mixing Electrospinning and Phase Inversion, *Polymers (Basel)*. 13 (2021) 790. <https://doi.org/10.3390/polym13050790>.

[22] L. Zheng, J. Wang, D. Yu, Y. Zhang, Y. Wei, Preparation of PVDF-CTFE hydrophobic membrane by non-solvent induced phase inversion: Relation between polymorphism and phase inversion, *Journal of Membrane Science*. 550 (2018). <https://doi.org/10.1016/j.memsci.2018.01.013>.

[23] B. Ameduri, From Vinylidene Fluoride (VDF) to the Applications of VDF-Containing Polymers and Copolymers: Recent Developments and Future Trends, *Chemical Reviews*. 109 (2009) 6632–86. <https://doi.org/10.1021/cr800187m>.

[24] M. Matsuda, K. Yamamoto, T. Yakushiji, M. Fukuda, T. Miyasaka, K. Sakai, Nanotechnological evaluation of protein adsorption on dialysis membrane surface hydrophilized with polyvinylpyrrolidone, *Journal of Membrane Science*. 310 (2008) 219–228. <https://doi.org/10.1016/j.memsci.2007.10.054>.

[25] X. Zhao, C. Liu, Irreversible fouling control of PVDF ultrafiltration membrane with “fouled surface” for mimetic sewage treatment, *RSC Adv*. 6 (2016) 94184–94192. <https://doi.org/10.1039/C6RA08292K>.

- [26] D. Hou, J. Wang, X. Sun, Z. Ji, Z. Luan, Preparation and properties of PVDF composite hollow fiber membranes for desalination through direct contact membrane distillation, (2012). <https://doi.org/10.1016/J.MEMSCI.2012.03.008>.
- [27] Y. Zhang, L. Ye, B. Zhang, Y. Chen, W. Zhao, G. Yang, J. Wang, H. Zhang, Characteristics and performance of PVDF membrane prepared by using NaCl coagulation bath: Relationship between membrane polymorphous structure and organic fouling, *Journal of Membrane Science*. 579 (2019) 22–32. <https://doi.org/10.1016/j.memsci.2019.02.054>.
- [28] I.M. Wienk, R.M. Boom, M.A.M. Beerlage, A.M.W. Bulte, C.A. Smolders, H. Strathmann, Recent advances in the formation of phase inversion membranes made from amorphous or semi-crystalline polymers, *Journal of Membrane Science*. 113 (1996) 361–371. [https://doi.org/10.1016/0376-7388\(95\)00256-1](https://doi.org/10.1016/0376-7388(95)00256-1).
- [29] F. Liu, N.A. Hashim, Y. Liu, M.R.M. Abed, K. Li, Progress in the production and modification of PVDF membranes, *Journal of Membrane Science*. 375 (2011) 1–27. <https://doi.org/10.1016/j.memsci.2011.03.014>.
- [30] J. Zhao, Development of polyvinylidene fluoride (PVDF) hollow fiber membranes by novel thermally induced phase separation, Thesis, 2019. <https://doi.org/10.32657/10220/47716>.
- [31] J. Drelich, E. Chibowski, D.D. Meng, K. Terpilowski, Hydrophilic and superhydrophilic surfaces and materials, *Soft Matter*. 7 (2011) 9804–9828. <https://doi.org/10.1039/C1SM05849E>.
- [32] T. Wu, H. Jin, S. Dong, X. Peng, H. Xu, L. Lu, Z. Fang, S. Huang, X. Tao, L. Shi, S. Liu, A Flexible Film Bulk Acoustic Resonator Based on α -Phase Polyvinylidene Fluoride Polymer, *Sensors*. 20 (2020) 1346. <https://doi.org/10.3390/s20051346>.
- [33] A.G. Fane, G. Chen, X. Yang, Y. Lu, R. Wang, Heat transfer intensification and scaling mitigation in bubbling-enhanced membrane distillation for brine concentration, (2014). <https://doi.org/10.1016/j.memsci.2014.07.017>.
- [34] H. Amii, K. Uneyama, C–F Bond Activation in Organic Synthesis, *Chemical Reviews*. 109 (2009) 2119–83. <https://doi.org/10.1021/cr800388c>.
- [35] N. Furusho, T. Komatsu, T. Nakagawa, A Study of the Thermal Degradation of Several Halogen-containing Polymers by Torsional Braid Analysis, *BCSJ*. 47 (1974) 1573–1577. <https://doi.org/10.1246/bcsj.47.1573>.
- [36] N.A.B. Hashim, Fabrication of Poly(Vinylidene Fluoride) (PVDF) Membranes, (2011). <https://doi.org/10.25560/6366>.
- [37] S.L. Madorsky, Thermal Degradation of Organic Polymers, Undefined. (1964). <https://www.semanticscholar.org/paper/Thermal-Degradation-of-Organic-Polymers-Madorsky/b364bf3f41da69d4ea8815a3e2966324266fad9e> (accessed April 11, 2022).
- [38] J.E. Dohany, Fluorine-containing polymers, poly (vinylidene fluoride), *Kirk-Othmer Encyclopedia of Chemical Technology*. (2000).

- [39] A. Lovinger, D. Reed, Inhomogeneous thermal degradation of poly (vinylidene fluoride) crystallized from the melt, *Macromolecules*. 13 (1980) 989–994.
- [40] H. Shinohara, Fluorination of polyhydrofluoroethylenes. II. Formation of perfluoroalkyl carboxylic acids on the surface region of poly(vinylidene fluoride) film by oxyfluorination, fluorination, and hydrolysis, *Journal of Polymer Science: Polymer Chemistry Edition*. 17 (1979) 1543–1556. <https://doi.org/10.1002/pol.1979.170170526>.
- [41] F. Vigo, C. Uliana, B. Cavazza, F. Salvemini, Mechanical, chemical and bacterial resistance of modified polyvinylidene fluoride membranes suitable for ultrafiltration of oily emulsions, *Journal of Membrane Science*. 21 (1984) 295–306. [https://doi.org/10.1016/S0376-7388\(00\)80220-3](https://doi.org/10.1016/S0376-7388(00)80220-3).
- [42] P. Jessop, The use of auxiliary substances (: E.g. solvents, separation agents) should be made unnecessary wherever possible and innocuous when used, *Green Chem*. 18 (2016). <https://doi.org/10.1039/C6GC90039A>.
- [43] M.L. Yeow, Y.T. Liu, K. Li, Isothermal phase diagrams and phase-inversion behavior of poly(vinylidene fluoride)/solvents/additives/water systems, *Journal of Applied Polymer Science*. 90 (2003) 2150–2155. <https://doi.org/10.1002/app.12846>.
- [44] M. Sadrzadeh, S. Bhattacharjee, Rational design of phase inversion membranes by tailoring thermodynamics and kinetics of casting solution using polymer additives, *Journal of Membrane Science*. 441 (2013) 31–44. <https://doi.org/10.1016/j.memsci.2013.04.009>.
- [45] M. Voronova, N. Rubleva, N. Kochkina, A. Afineevskii, A. Zakharov, O. Surov, Preparation and characterization of polyvinylpyrrolidone/cellulose nanocrystals composites, *Nanomaterials*. 8 (2018) 1011.
- [46] K.M. Koczur, S. Mourdikoudis, L. Polavarapu, S.E. Skrabalak, Polyvinylpyrrolidone (PVP) in nanoparticle synthesis, *Dalton Transactions*. 44 (2015) 17883–17905.
- [47] B.J. Cha, J.M. Yang, Effect of high-temperature spinning and PVP additive on the properties of PVDF hollow fiber membranes for microfiltration, *Macromol. Res*. 14 (2006) 596–602. <https://doi.org/10.1007/BF03218730>.
- [48] Z.A. Parray, M.I. Hassan, F. Ahmad, A. Islam, Amphiphilic nature of polyethylene glycols and their role in medical research, *Polymer Testing*. 82 (2020) 106316. <https://doi.org/10.1016/j.polymertesting.2019.106316>.
- [49] B. Ensing, A. Tiwari, M. Tros, J. Hunger, S.R. Domingos, C. Pérez, G. Smits, M. Bonn, D. Bonn, S. Woutersen, On the origin of the extremely different solubilities of polyethers in water, *Nat Commun*. 10 (2019) 2893. <https://doi.org/10.1038/s41467-019-10783-z>.
- [50] H. Zhang, X. Lu, Z. Liu, Z. Ma, S. Wu, Z. Li, X. Kong, C. Wu, Study of the dual role mechanism of water-soluble additive in low temperature thermally-induced phase separation, *Journal of Membrane Science*. 543 (2017) 1–9. <https://doi.org/10.1016/j.memsci.2017.08.032>.

- [51] Q. Zhang, X. Lu, L. Zhao, Preparation of polyvinylidene fluoride (PVDF) hollow fiber hemodialysis membranes, *Membranes*. 4 (2014) 81–95.
- [52] J.-F. Huang, S.-J. Han, H.-J. Chen, G.-S. Liu, G.-T. Li, Y.-C. Wang, Z.-X. Wang, B.-R. Yang, Z.-H. Luo, H.-P.D. Shieh, Enhancement of polar phases in PVDF by forming PVDF/SiC nanowire composite, *IEEE Transactions on Dielectrics and Electrical Insulation*. 23 (2016) 3612–3619.
- [53] J. Meyer, PVDF Ultrafiltrationsmembranen mit maßgeschneiderter Trennleistung durch Einsatz von PEO-b-PMMA Diblock Copolymeren, (2018). https://duepublico2.uni-due.de/receive/duepublico_mods_00046009 (accessed March 28, 2022).
- [54] J. Schmitt, H.-C. Flemming, FTIR-spectroscopy in microbial and material analysis, *International Biodeterioration & Biodegradation*. 41 (1998) 1–11.
- [55] D.Y. Kwok, A.W. Neumann, Contact angle measurement and contact angle interpretation, *Advances in Colloid and Interface Science*. 81 (1999) 167–249.
- [56] A. Kota, G. Kwon, A. Tuteja, The design and applications of superomniphobic surfaces, *NPG Asia Materials*. 6 (2014) e109. <https://doi.org/10.1038/am.2014.34>.
- [57] S. Laurén, How to measure contact angle hysteresis?, (n.d.). <https://www.biolinscientific.com/blog/how-to-measure-contact-angle-hysteresis> (accessed April 17, 2022).
- [58] B. Ma, J. Yang, Q. Sun, W. Jakpa, X. Hou, Y. Yang, Influence of cellulose/[Bmim]Cl solution on the properties of fabricated NIPS PVDF membranes, *Journal of Materials Science*. 52 (2017) 9946–9957. <https://doi.org/10.1007/s10853-017-1150-2>.
- [59] R.A. Lusiana, A. Indra, N.B.A. Prasetya, N.A. Sasongko, P. Siahaan, C. Azmiyawati, N. Wijayanti, A.R. Wijaya, M.H.D. Othman, The Effect of Temperature, Sulfonation, and PEG Addition on Physicochemical Characteristics of PVDF Membranes and Its Application on Hemodialysis Membrane, *Indonesian Journal of Chemistry*. 21 (2021) 942–953. <https://doi.org/10.22146/ijc.63740>.
- [60] V. Kumar, P. Kumar, A. Nandy, P.P. Kundu, A nanocomposite membrane composed of incorporated nano-alumina within sulfonated PVDF-co-HFP/Nafion blend as separating barrier in a single chambered microbial fuel cell, *RSC Adv*. 6 (2016) 23571–23580. <https://doi.org/10.1039/C6RA03598A>.
- [61] E. Popek, Chapter 4 - Practical Approach to Sampling, in: E. Popek (Ed.), *Sampling and Analysis of Environmental Chemical Pollutants (Second Edition)*, Elsevier, 2018: pp. 145–225. <https://doi.org/10.1016/B978-0-12-803202-2.00004-5>.
- [62] L.L. Simon, E. Simone, K. Abbou Oucherif, Chapter 9 - Crystallization process monitoring and control using process analytical technology, in: R. Singh, Z. Yuan (Eds.), *Computer Aided Chemical Engineering*, Elsevier, 2018: pp. 215–242. <https://doi.org/10.1016/B978-0-444-63963-9.00009-9>.

- [63] C.N. Sawyer, P.L. McCarty, G.F. Parkin, *Chemistry for environmental engineering and science*. (5th ed.), McGraw-Hill, 2003. http://repository.vnu.edu.vn/handle/VNU_123/90733 (accessed October 21, 2022).
- [64] A. Volkov, *Membrane Compaction*, in: 2014: pp. 1–2. https://doi.org/10.1007/978-3-642-40872-4_1404-2.
- [65] I. Ali, O.A. Bamaga, L. Gzara, M. Bassyouni, M.H. Abdel-Aziz, M.F. Soliman, E. Drioli, M. Albeirutty, *Assessment of Blend PVDF Membranes, and the Effect of Polymer Concentration and Blend Composition*, *Membranes*. 8 (2018) 13. <https://doi.org/10.3390/membranes8010013>.
- [66] X.-Y. Xing, L. Gu, Y. Jin, R. Sun, M.-Y. Xie, Q.-Y. Wu, *Fabrication and characterization of cellulose triacetate porous membranes by combined nonsolvent-thermally induced phase separation*, *Cellulose*. 26 (2019) 3747–3762. <https://doi.org/10.1007/s10570-019-02347-7>.
- [67] E.-S. Kim, G. Hwang, M.G. El-Din, Y. Liu, *Development of nanosilver and multi-walled carbon nanotubes thin-film nanocomposite membrane for enhanced water treatment*, *Journal of Membrane Science. Complete* (2012) 37–48. <https://doi.org/10.1016/j.memsci.2011.11.041>.
- [68] H. Bai, X. Wang, Y. Zhou, L. Zhang, *Preparation and characterization of poly(vinylidene fluoride) composite membranes blended with nano-crystalline cellulose*, *Progress in Natural Science: Materials International*. 22 (2012) 250–257. <https://doi.org/10.1016/j.pnsc.2012.04.011>.
- [69] H. Abdolmaleki, S. Agarwala, *PVDF-BaTiO₃ Nanocomposite Inkjet Inks with Enhanced β -Phase Crystallinity for Printed Electronics*, *Polymers*. 12 (2020) 2430. <https://doi.org/10.3390/polym12102430>.
- [70] I. Purnawan, D. Angputra, S.C. Debora, E.F. Karamah, A. Febriasari, S. Kartohardjono, *Polyvinylidene Fluoride Membrane with a Polyvinylpyrrolidone Additive for Tofu Industrial Wastewater Treatment in Combination with the Coagulation–Flocculation Process*, *Membranes*. 11 (2021) 948. <https://doi.org/10.3390/membranes11120948>.
- [71] Z. Zeng, D. Yu, Z. He, J. Liu, F.-X. Xiao, Y. Zhang, R. Wang, D. Bhattacharyya, T.T.Y. Tan, *Graphene Oxide Quantum Dots Covalently Functionalized PVDF Membrane with Significantly-Enhanced Bactericidal and Antibiofouling Performances*, *Sci Rep*. 6 (2016) 20142. <https://doi.org/10.1038/srep20142>.
- [72] X. Cai, T. Lei, D. Sun, L. Lin, *A critical analysis of the α , β and γ phases in poly(vinylidene fluoride) using FTIR*, *RSC Advances*. 7 (2017) 15382–15389. <https://doi.org/10.1039/C7RA01267E>.
- [73] Z. Guo, X. Xu, Y. Xiang, S. Lu, S.P. Jiang, *New anhydrous proton exchange membranes for high-temperature fuel cells based on PVDF–PVP blended polymers*, *J. Mater. Chem. A*. 3 (2014) 148–155. <https://doi.org/10.1039/C4TA04952G>.
- [74] N. Chen, L. Hong, *Surface phase morphology and composition of the casting films of PVDF–PVP blend*, *Polymer*. 43 (2002) 1429–1436. [https://doi.org/10.1016/S0032-3861\(01\)00671-1](https://doi.org/10.1016/S0032-3861(01)00671-1).

- [75] M. Mertens, M.R. Bilad, A.Y. Gebreyohannes, L. Marbelia, I.F.J. Vankelecom, Membrane development for improved performance of a magnetically induced vibration system for anaerobic sludge filtration, *Separation and Purification Technology*. 200 (2018) 120–129. <https://doi.org/10.1016/j.seppur.2018.01.068>.
- [76] N.I. Mat Nawi, H.M. Cean, N. Shamsuddin, M.R. Bilad, T. Narkkun, K. Faungnawakij, A.L. Khan, Development of Hydrophilic PVDF Membrane Using Vapour Induced Phase Separation Method for Produced Water Treatment, *Membranes*. 10 (2020) 121. <https://doi.org/10.3390/membranes10060121>.
- [77] Syawaliah, N. Arahman, Mukramah, S. Mulyati, Effects of PEG Molecular Weights on PVDF Membrane for Humic Acid-fed Ultrafiltration Process, *IOP Conf. Ser.: Mater. Sci. Eng.* 180 (2017) 012129. <https://doi.org/10.1088/1757-899X/180/1/012129>.
- [78] P.D. Lewis, K.E. Lewis, R. Ghosal, S. Bayliss, A.J. Lloyd, J. Wills, R. Godfrey, P. Kloer, L.A. Mur, Evaluation of FTIR Spectroscopy as a diagnostic tool for lung cancer using sputum, *BMC Cancer*. 10 (2010) 640. <https://doi.org/10.1186/1471-2407-10-640>.
- [79] T. Marino, F. Russo, A. Figoli, The Formation of Polyvinylidene Fluoride Membranes with Tailored Properties via Vapour/Non-Solvent Induced Phase Separation, *Membranes*. 8 (2018) 71. <https://doi.org/10.3390/membranes8030071>.
- [80] A. Febriasari, Huriya, A.H. Ananto, M. Suhartini, S. Kartohardjono, Polysulfone–Polyvinyl Pyrrolidone Blend Polymer Composite Membranes for Batik Industrial Wastewater Treatment, *Membranes*. 11 (2021) 66. <https://doi.org/10.3390/membranes11010066>.
- [81] Z. Zheng, Z. Gu, R. Huo, Y. Ye, Superhydrophobicity of polyvinylidene fluoride membrane fabricated by chemical vapor deposition from solution, *Applied Surface Science*. 255 (2009) 7263–7267. <https://doi.org/10.1016/j.apsusc.2009.03.084>.
- [82] Bioinspired Poly(vinylidene fluoride) Membranes with Directional Release of Therapeutic Essential Oils | *Langmuir*, (n.d.). <https://pubs.acs.org/doi/10.1021/acs.langmuir.8b01175> (accessed December 15, 2022).
- [83] T.T.V. Tran, S.R. Kumar, C.H. Nguyen, J.W. Lee, H.-A. Tsai, C.-H. Hsieh, S.J. Lue, High-permeability graphene oxide and poly(vinyl pyrrolidone) blended poly(vinylidene fluoride) membranes: Roles of additives and their cumulative effects, *Journal of Membrane Science*. 619 (2021) 118773. <https://doi.org/10.1016/j.memsci.2020.118773>.
- [84] N.A. Ochoa, M. Masuelli, J. Marchese, Effect of hydrophilicity on fouling of an emulsified oil wastewater with PVDF/PMMA membranes, *Journal of Membrane Science*. 226 (2003) 203–211. <https://doi.org/10.1016/j.memsci.2003.09.004>.
- [85] B.S. Lalia, V. Kochkodan, R. Hashaikheh, N. Hilal, A review on membrane fabrication: Structure, properties and performance relationship, *Desalination*. 326 (2013) 77–95. <https://doi.org/10.1016/j.desal.2013.06.016>.

- Appendixes

Appendix A: Pore dimension measurement of fabricated membranes.

All the measurements were not presented in hard copy but saved in Appendix A in STAG due to the bulky of the measurement data.

Appendix B: Membrane thickness measurement of fabricated membranes.

Table 0-1 Thickness measurement of PVDF10.

	Membrane thickness (in nanometer)
1	32201.029
2	27837.138
3	28876.082
4	25604.26
5	23879.908
6	26327.861
7	24286.056
8	27651.006

Table 0-2 Thickness measurement of PVDF10/PVP2.

	Membrane thickness (in nanometer)
1	37730.771
2	45590.265
3	41474.557
4	40637.284
5	34570.781
6	34258.008
7	37950.992
8	32414.417

Table 0-3 Thickness measurement of PVDF10/PVP5.

	Membrane thickness (in nanometer)
1	87714.751
2	77327.821
3	77433.316
4	77748.942
5	74996.599
6	84103.92

7	90756.458
8	75281.784
9	78623.359
10	74792.229
11	92317.111

Table 0-4 Thickness measurement of PVDF10/PVP8.

	Membrane thickness (in nanometer)
1	115401.821
2	108177.897
3	118870.71
4	115573.69
5	120999.305
6	112522.21
7	108985.7

Table 0-5 Thickness measurement of PVDF10/PEG2.

	Membrane thickness (in nanometer)
1	65434.186
2	52702.476
3	52450.171
4	47745.071
5	46097.722
6	41286.703
7	43990.955
8	49057.442

Table 0-6 Thickness measurement of PVDF10/PEG5.

	Membrane thickness (in nanometer)
1	42738.916
2	40868.684
3	37650.235
4	36439.454
5	36533.747
6	34847.829
7	40049.969
8	38047.208

Table 0-7 Thickness measurement of PVDF10/PEG8.

	Membrane thickness (in nanometer)
1	61674.021
2	59547.138
3	61666.667
4	63349.443
5	68816.114
6	67669.75
7	63831.286
8	68337.066

Table 0-8 Thickness measurement of PVDF15.

	Membrane thickness (in nanometer)
1	64845.971
2	63505.905
3	69079.664
4	66483.081
5	64078.077
6	61269.895
7	64474.801
8	64621.978
9	62649.82

Table 0-9 Thickness measurement of PVDF15/PVP2.

	Membrane thickness (in nanometer)
1	26496.214
2	29868.022
3	33098.805
4	36233.127
5	34250.529
6	31522.675
7	30823.472
8	33074.924
9	32081.878
10	29410.882

Table 0-10 Thickness measurement of PVDF15/PVP5.

	Membrane thickness (in nanometer)
1	73871.941
2	78827.98
3	93168.302
4	92637.56
5	94008.899
6	100138.408
7	91578.947
8	122368.138
9	105394.655
10	118737.589
11	106362.679
12	115372.455
13	102473.563

Table 0-11 Thickness measurement of PVDF15/PVP8.

	Membrane thickness (in nanometer)
1	156405.62
2	169820.716
3	135360.08
4	148318.886
5	125070.675
6	127117.503
7	114836.513
8	116985.71
9	117521.642
10	119491.204
11	125160.364

Table 0-12 Thickness measurement of PVDF15/PEG2.

	Membrane thickness (in nanometer)
1	31693.945
2	33841.497
3	34231.24
4	33541.756
5	31353.225
6	32855.839
7	30115.006

8	33596.921
9	33206.611
10	33943.49

Table 0-13 Thickness measurement of PVDF15/PEG5.

	Membrane thickness (in nanometer)
1	55916.163
2	56205.97
3	57318.689
4	56617.408
5	56011.022
6	55667.443
7	52988.235
8	51763.947

Table 0-14 Thickness measurement of PVDF15/PEG8.

	Membrane thickness (in nanometer)
1	59410.913
2	59704.44
3	59704.44
4	59578.82
5	60480.215
6	54774.156
7	54682.891
8	55498.873

Table 0-15 Thickness measurement of PVDF20.

	Membrane thickness (in nanometer)
1	44600.73
2	46541.368
3	46735.595
4	48690.533
5	48248.426
6	44953.994
7	47178.576
8	46369.896
9	47828.006

Table 0-16 Thickness measurement of PVDF20/PVP2.

	Membrane thickness (in nanometer)
1	28165.846
2	27611.241
3	27574.874
4	28055.555
5	27202.941
6	26574.958
7	24941.454
8	26435.009

Table 0-17 Thickness measurement of PVDF20/PVP5.

	Membrane thickness (in nanometer)
1	110006.313
2	105491.574
3	108448.657
4	106301.458
5	102432.227
6	90588.355
7	106930.013
8	93370.528
9	97314.639

Table 0-18 Thickness measurement of PVDF20/PVP8.

	Membrane thickness (in nanometer)
1	198761.598
2	190029.238
3	186752.626
4	182743.158
5	167128.988
6	167128.988
7	152550.336
8	161493.798
9	150000
10	141639.431

Table 0-19 Thickness measurement of PVDF20/PEG2.

	Membrane thickness (in nanometer)
1	44066.971
2	44895.57
3	45434.187
4	44157.649
5	46312.382
6	42078.644
7	41155.256
8	42075.976

Table 0-20 Thickness measurement of PVDF20/PEG5.

	Membrane thickness (in nanometer)
1	79707.871
2	81195.713
3	77183.998
4	76533.825
5	82989.085
6	72357.844
7	80486.756

Table 0-21 Thickness measurement of PVDF20/PEG8.

	Membrane thickness (in nanometer)
1	71494.973
2	70005.401
3	71839.521
4	72526.965
5	72149.354
6	72195.518
7	69653.816
8	64986.912